

Nutrient release and flux dynamics of CO₂, CH₄, and N₂O in a coastal peatland driven by actively induced rewetting with brackish water from the Baltic Sea

Daniel Lars Pönisch^{1*}, Anne Breznikar^{2*}, Cordula Nina Gutekunst³, Gerald Jurasinski³, Maren Voss²,

5 Gregor Rehder¹

* these authors contributed equally to this work and share first authorship

¹ Department of Marine Chemistry, Leibniz Institute for Baltic Sea Research Warnemünde (IOW), Rostock, Germany

² Department of Biological Oceanography, Leibniz Institute for Baltic Sea Research Warnemünde (IOW), Rostock, Germany

³ Department of Landscape Ecology, Faculty for Agriculture and Environmental Sciences, University of Rostock, Germany

10 Correspondence to: Daniel L. Pönisch (daniel.poenisch@io-warnemuende.de) and Anne Breznikar (anne.breznikar@io-warnemuende.de)

Abstract. The rewetting of drained peatlands supports long-term nutrient removal in addition to reducing emissions of carbon dioxide (CO₂) and nitrous oxide (N₂O). However, rewetting may lead to short-term nutrient leaching into adjacent water and high methane (CH₄) emissions. The consequences of rewetting with brackish water on nutrient and greenhouse gas 15 (GHG) fluxes remain unclear, although beneficial effects such as lower CH₄ emissions seem likely. Therefore, we studied the actively induced rewetting of a coastal peatland with brackish water, by comparing pre- and post-rewetting data from the peatland and the adjacent bay.

Both the potential transport of nutrients into adjacent coastal water and the shift of GHG fluxes (CO₂, CH₄, N₂O) accompanying the change from drained to inundated conditions were analyzed based on measurements of the surface water 20 concentrations of nutrients (dissolved inorganic nitrogen (DIN), phosphate (PO₄³⁻)), oxygen (O₂), components of the CO₂ system, CH₄, and N₂O together with manual closed-chamber measurements of GHG fluxes.

Our results revealed higher nutrient concentrations in the rewetted peatland than in the adjacent bay, indicating that nutrients leached out of the peat and were exported to the bay. A comparison of DIN concentrations of the bay with those of an unaffected reference station showed a significant increase after rewetting. The maximum estimated nutrient export out of 25 the peatland was calculated to be 33.8 ± 9.6 t yr⁻¹ for DIN-N and 0.24 ± 0.29 t yr⁻¹ for PO₄-P, depending on the endmember (bay vs. reference station).

The peatland was also a source of GHG in the first year after rewetting. However, the spatial and temporal variability decreased and high CH₄ emissions, as reported for freshwater rewetting, did not occur. CO₂ fluxes decreased slightly from 0.29 ± 0.82 g m⁻² h⁻¹ (pre-rewetting) to 0.26 ± 0.29 g m⁻² h⁻¹ (post-rewetting). The availability of organic 30 matter (OM) and dissolved nutrients were likely the most important drivers of continued CO₂ production. Pre-rewetting CH₄ fluxes ranged from 0.13 ± 1.01 mg m⁻² h⁻¹ (drained land site) to 11.4 ± 37.5 mg m⁻² h⁻¹ (ditch). After rewetting, CH₄ fluxes

on the formerly dry land increased by 1 order of magnitude ($1.74 \pm 7.59 \text{ mg m}^{-2} \text{ h}^{-1}$), whereas fluxes from the former ditch decreased to $8.5 \pm 26.9 \text{ mg m}^{-2} \text{ h}^{-1}$. These comparatively low CH_4 fluxes can likely be attributed to the suppression of methanogenesis by the available O_2 and sulfate, which serve as alternative electron acceptors. The post-rewetting N_2O flux 35 was low, with an annual mean of $0.02 \pm 0.07 \text{ mg m}^{-2} \text{ h}^{-1}$.

Our results suggest that rewetted coastal peatlands could account for high, currently unmonitored nutrient inputs into adjacent coastal water, at least on a short time scale such as a few years. However, rewetting with brackish water may decrease GHG emissions and might be favored over freshwater rewetting in order to reduce CH_4 emissions.

1. Introduction

40 Pristine peatlands are natural sinks for nutrients, in particular nitrate (NO_3^-), and greenhouse gases (GHG) such as carbon dioxide (CO_2) and nitrous oxide (N_2O) (Strack, 2008; Kaat and Joosten, 2009). Globally, peatlands store up to 550 Gt of carbon (C), which is twice the C stock of total forest biomass (Moore et al., 1998; Joosten and Clarke, 2002; Kaat and Joosten, 2009).

45 The drainage of peatlands leads to the mineralization of the topmost peat layer and the accumulation of nutrients (Cabezas et al., 2012). After rewetting, peatlands can therefore be sources of nutrients, especially ammonium (NH_4^+) and phosphate (PO_4^{3-}) (Lamers et al., 2002; Cabezas et al., 2012; Duhamel et al., 2017). Conversely, due to the anoxic conditions in the water-saturated peat, rewetted peatlands can also act as nutrient sinks, mainly for NO_3^- (Fisher and Acreman, 2004). Whether rewetting leads to nutrient release or uptake is, besides other factors, controlled by the degree of peat decomposition (Zak and Gelbrecht, 2007; Cabezas et al., 2012), the water level (Duhamel et al., 2017) and the salinity (Liu and Lennartz, 50 2019). Nutrient release is highest in strongly degraded peat in formerly drained peatlands (Zak and Gelbrecht, 2007; Cabezas et al., 2012). Therefore, removal of the topsoil before rewetting has been recommended as a measure to greatly reduce the release of PO_4^{3-} and nitrogen (N) (Harpenslager et al., 2015; Zak et al., 2017). However, nutrient release from peat after rewetting has mostly been assessed in laboratory and incubation studies. To our knowledge, field data on nutrient leaching and potential exports to adjacent waters are lacking.

55 The GHG exchange of peatlands is strongly influenced by the prevailing biogeochemical and physical conditions, which in turn are largely determined by vegetation and the water level and thus the ratio of oxic and anoxic conditions (Kaat and Joosten, 2009). In drained peatlands, the low water table enables the aerobic decomposition of peat, which is accompanied by increased CO_2 emissions (Joosten and Clarke, 2002). In rewetted peatlands, CO_2 emissions are regulated by photosynthesis, decomposition, and temperature within the upper oxygen-rich soil layer and the overlying water column (Parish, 2008; Oertel et al., 2016). In the anoxic water-saturated zones, the formerly oxygen-induced decomposition of 60 organic matter (OM) is slowed and relies on alternative terminal electron acceptors (TEAs) such as NO_3^- , manganese (Mn^{4+}), iron (Fe^{3+}), and sulfate (SO_4^{2-}), leading to lowered CO_2 emissions (Strack, 2008; Dean et al., 2018). However,

methanogenesis, as the last step in the mineralization of OM and a depletion of TEAs, may become more important in anoxic zones.

65 Methane (CH_4) emissions in drained peatlands are virtually negligible at water levels < 20 cm below the surface (Jurasinski et al., 2016). Although CH_4 is formed in anoxic zones via methanogenesis, most of it is oxidized as it passes through the oxic soil layer (Kaat and Joosten, 2009; Dean et al., 2018). Consequently, drained peatlands are a minor source of atmospheric CH_4 . In rewetted peatlands, CH_4 is microbially produced in water-saturated, anoxic soil layers mainly by archaea, when all other TEAs are depleted (Schönheit et al., 1982; Oremland, 1988; Segers and Kengen, 1998), so rewetted 70 peatlands are often significant sources of CH_4 (Hahn et al., 2015). However, in coastal peatlands that receive marine water and therefore SO_4^{2-} , the contribution of methanogenesis might be reduced, as methanogenic archaea are outcompeted by sulfate-reducing bacteria (SRB) (Bartlett et al., 1987; Capone and Kiene, 1988; Oremland, 1988; Jørgensen, 2006). Additionally, any CH_4 produced may be oxidized by anaerobic methane oxidation coupled to SO_4^{2-} reduction (e.g. Boetius et al., 2000).

75 N_2O is an intermediate in microbial processes, mostly nitrification, denitrification and nitrifier-denitrification (Kool et al., 2011). In degraded peatlands, all of these processes are fueled by the accumulated nutrients. Drained peatlands can be weak (Martikainen et al., 1993) or strong sources of N_2O (Liu et al., 2019), depending mainly on the climate zone and land use (Petersen et al., 2012; Leppelt et al., 2014). Rewetted, and thus water-saturated, peat usually acts as N_2O sink over long-term scales, due to the formation of anoxic zones where N_2O is consumed (Strack, 2008). However, rewetting can increase 80 the N_2O production and thus its release into the atmosphere due to the high nutrient availability in strongly degraded peat, which enables higher rates of nitrification and denitrification (Moseman-Valtierra et al., 2011; Chmura et al., 2016; Roughan et al., 2018).

In temperate latitudes, coastal peatlands are widespread at the interface between marine and terrestrial ecosystems. However, for many coastal peatlands, the sinking of their ground level due to degradation and peat shrinkage over decades 85 has made them vulnerable to rising sea level and sinking coasts (Jurasinski et al., 2018). In Mecklenburg-Vorpommern (northeastern Germany), currently drained coastal peatlands along the low-lying coastline cover an area of ~ 360 – 400 km^2 (Bockholt, 1985; Holz et al., 1996). Nowadays, peatlands are rewetted to restore their habitat function and biodiversity, thereby preventing CO_2 and N_2O emissions and, in the long-term, reestablishing their C- and N-storage capacity (Strack, 2008; Zielinski et al., 2018).

90 Coastal drained peatlands may be rewetted in different ways depending on the available water source. The rewetting can consist of permanent flooding with freshwater (from groundwater or rivers), episodical inundations with brackish water and permanent brackish water flooding. While the effects of freshwater rewetting (Richert et al., 2000; Hogan et al., 2004; Zak and Gelbrecht, 2007) and episodical inundations with brackish water on nutrient dynamics and GHG have been investigated (Chmura et al., 2011; Neubauer et al., 2013; Hahn et al., 2015; Koepsch et al., 2019), less is known about the 95 impact of permanent brackish water flooding.

In this study we examined the immediate effects of rewetting with brackish water on nutrient (NO_3^- , nitrite (NO_2^-), NH_4^+ and PO_4^{3-}) and GHG fluxes (CO_2 , CH_4 , N_2O) in a low-lying, highly degraded coastal peatland at the German Baltic Sea coast, by comparing pre- and post-rewetting conditions. Due to the unique formation of a permanent brackish water column above formerly drained peat, this is the first study to combine marine shallow-water and terrestrial peatland research.

100 We investigated how the rewetting with brackish water affects (1) nutrient leaching and the potential transport from a nutrient-enriched, flooded peatland to the adjacent bay driven by frequent water exchange, (2) the GHG dynamics in the surface water within the first year after rewetting and (3) the GHG fluxes along the transition from drained to inundated conditions.

2. Material and methods

105 2.1 Study area

The study area is a low-lying, highly degraded coastal peatland that had been transformed from a drained, agriculturally used polder to a brackish wetland. The “Polder Drammendorf” (referred to in the following as “peatland”) is located at the northeastern German Baltic Sea coast, on the western part of the island of Rügen (Mecklenburg-Vorpommern, Germany), bordering on the Kubitzer Bodden (Figure 1). The climate is oceanic, with a mean annual air temperature of 9.1°C and a

110 mean annual precipitation height of 626 mm (Deutscher Wetterdienst (DWD), 1991–2020). The central Kubitzer Bodden has a mean surface water temperature of $11.4 \pm 6.6^\circ\text{C}$ and a mean surface salinity of 8.5 ± 1.4 (referred to in the following as “central bay”, data retrieved from a monitoring station of the Landesamt für Umwelt, Naturschutz und Geologie Mecklenburg Vorpommern (LUNG MV), 2006–2020, 54.40°N , 13.11°E , Figure 1b). For comparison, the Arkona Basin, a

115 near-by open Baltic Sea basin, has a mean surface water temperature of $10.2 \pm 5.6^\circ\text{C}$ and a mean surface salinity of 8.0 ± 0.5 (MARNET, data originator: Leibniz Institute for Baltic Sea Research Warnemünde, Germany, 2006–2020, 54.88°N , 13.86°E).

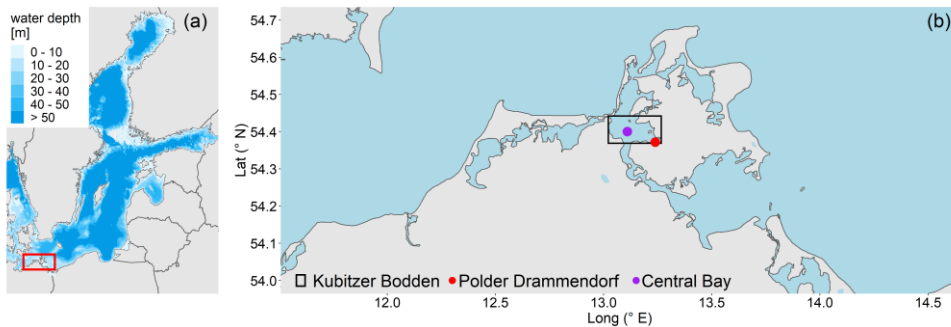
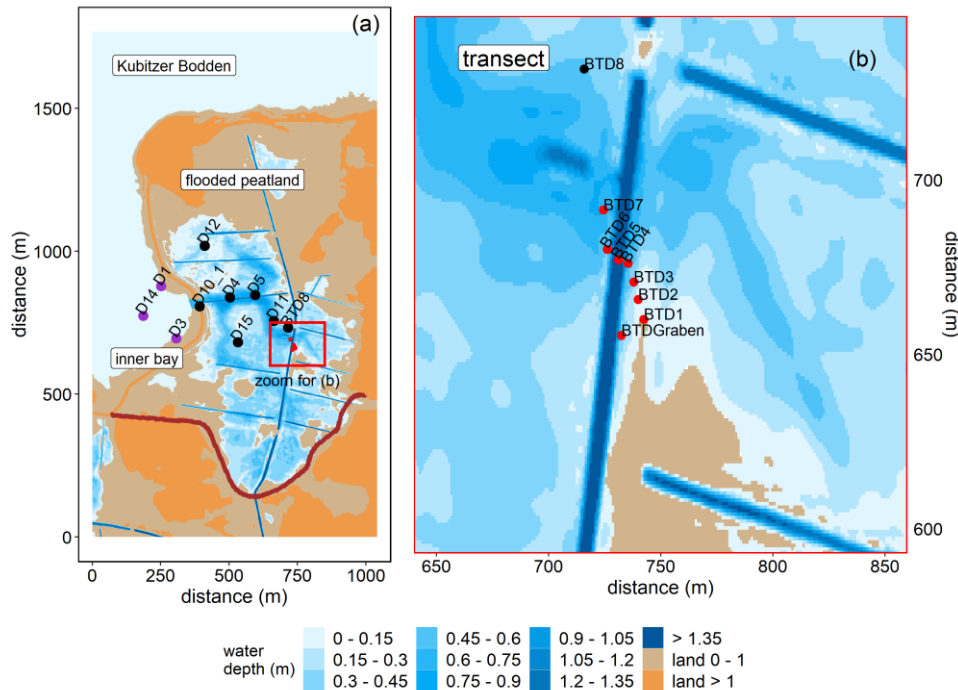


Figure 1. (a) Overview of the study area located in the southern Baltic Sea. (b) Coastline of northeast Germany in Mecklenburg-Vorpommern and study area location (“*Polder Drammendorf*”, red) on the island of Rügen, bordering on the Kubitzer Bodden, where a monitoring station served as reference (“central bay”, purple). Data retrieved from EEA, NOAA.

120

Like most peatlands in northern Germany, Drammendorf was artificially drained for agricultural use (pasture and grassland) in the 1960s, by establishing a sandy dike and an extensive ditch system that affected an area of 2.2 km². The northwestern part (mostly mineral soil, higher elevation) served as grassland while the northeastern part was used for agriculture with seasonal fertilizer application only until the 1990s (10 t N km⁻² yr⁻¹). The southern compartment (organic soil) provided an area for cattle grazing (~30 cows). The topsoil of the central part consists of up to 50–70 cm highly degraded peat (Brisch, 2015), classified as H7 according to the von Post humification scale (Wang et al., 2021). This highly degraded topsoil layer was not removed prior to rewetting. Underneath the degraded topsoil follows a well-preserved peat layer with a thickness of ~100 cm. Peat deposits of up to 220 cm thickness are largest in the western part, near the former dike. The long-lasting drainage and ongoing peat degradation have led to the formation of a local land depression with an average soil elevation of around –0.5 meters above sea level (masl). To control the water expansion after rewetting, a new dike was built in the southern part before flooding (Figure 2a). Additionally, a drainage ditch that receives water from the catchment was rebuilt and a new pumping station was installed. A significant input of nutrients from this additional water supply can be excluded due to the low pumping activity and the absence of a permanent hydrological connection to the study area (Wasser- und Bodenverband Rügen (WBV), pers. comm., 2020).



135 **Figure 2.** Topography of the study area and overview of the stations in the inner bay (purple), the flooded peatland (black) and along the transect [of the GHG flux measurements](#) (red). (a) Water coverage at mean sea level. The new dike is shown in dark red. (b) Transect stations that were sampled for atmospheric chamber-based GHG flux measurements (before and after rewetting) and for surface water GHG concentration measurements (after rewetting). Data from station BTD7 were used for a comparison of the chamber-based measurements with the calculated air-sea fluxes after rewetting. Topography data retrieved from AfGVK, LAiV MV.

140

The area was rewetted by the targeted removal of a 20 m wide dike section in November 2019 that caused an immediate flooding of the low-lying area behind the dike. The newly built channel represents the only permanent hydrological connection between the peatland and the Kubitzer Bodden that allows major surface water exchange. The remaining section of the dike (~650 m) was removed down to the surface elevation level and is hence only flooded at very high water levels.

145

The restored area covers ~0.8 km² in total and is characterized by a permanently water-covered area of ~0.5 km², with a mean water depth of ~0.5 m, compared to 1.0–1.5 m in the Kubitzer Bodden. The extent of the inundated area depends directly on the water level of the Baltic Sea, which is highly dynamic despite the absence of regular tides (Figure A1). Therefore, minor changes in the water level lead to major changes in the water-covered area. For instance, if the water level rises from −0.5 to + 0.5 masl, the water-covered area increases from 0.08 to 0.7 km² (Figure 3, Figure A2). [The ditch](#)

150 system was only partly removed and hence, some deeper areas with water depths of up to 4 m remained. It is noteworthy that in the first months after rewetting, former grassland and ditch vegetation (*Elymus repens* L. (Gould) (Couch grass), *Phragmites australis* (Cav.) Trin. ex Steud. (Common reed)) died almost completely and the cover of emergent macrophytes was then negligible. However, *Phragmites* was able to grow back during the growing season and expanded especially around the ditches.

155

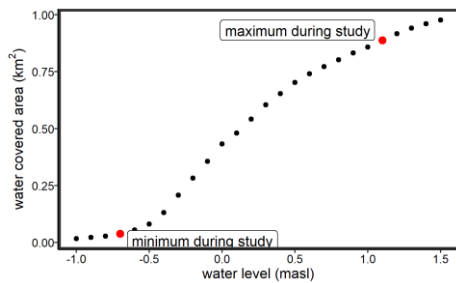


Figure 3. Hypsographic curve of the study area, in increments of 0.1 m. The red dots represent the observed range of the water level during the study. For a water level time series during the sampling period, see Figure A1.

2.2 Sampling

2.2.1 Surface water sampling

160 Before rewetting, surface water samples for nutrients (NO_3^- , NO_2^- , NH_4^+ , PO_4^{3-}) and chlorophyll a were collected from the inner Kubitzer Bodden (referred to in the following as “inner bay”) at station D1 (Figure 2a) and irregularly at a second station right in front of the now removed dike section, which was abandoned after rewetting and therefore merged with station D1. Both stations were reached from land and sampling was conducted monthly from June to November 2019, except in August.

165 After rewetting, surface water samples were collected with a small boat and the sampled variables were extended for the concentrations of GHGs (CO_2 , CH_4 , N_2O) and dissolved organic carbon (DOC). The first sampling took place one week after the dike removal. Sampling was continued over one year (25 sampling dates until December 2020) at weekly (December 2019 to January 2020) or biweekly (February 2020 to September 2020, except for August) intervals. From October 2020 to December 2020, sampling was conducted monthly. In the inner bay, three stations (D1, D3, D14), and in the 170 flooded peatland six stations (D4, D5, D11, D12, D15, BTD8) were sampled (Figure 2a). The inner bay station “D14” was sampled from March 2020 onwards. DOC sampling started in April 2020. For the air-sea gas exchange calculation, data from station D10_1, located in the channel, were also included.

Gelöscht: The ditch system and its surrounding vegetation (*Elymus repens* L. (Gould) (Couch grass), *Phragmites australis* (Cav.) Trin. ex Steud. (Common reed)) were only partly removed. Hence, some deeper areas with water depths of up to 4 m remained.

Moreover, surface water samples for the analysis of GHG concentrations (CO_2 , CH_4 , N_2O) were sampled at eight stations along a transect (Figure 2b). This sampling was carried out simultaneously with the sampling described in Sect. 2.2.2 to link GHG air-sea exchange calculations based on surface water samples with chamber-based flux measurements.

180 Surface water temperature, dissolved oxygen (O_2), and salinity were measured directly in the field using a HACH HQ40D multimeter (HACH Lange GmbH, Germany) equipped with two outdoor electrodes (LDO10105, CDC40105). Depending on the prevailing water depth, additional measurements were conducted in the peatland 15 cm above the soil surface (excluding the ditches) on 22 of the 25 sampling dates. The precision of the electrodes was $\pm 0.3^\circ\text{C}$, $\pm 0.8\%$, and ± 0.1 for temperature, O_2 saturation, and salinity, respectively.

185 Surface water samples were taken using a horizontal 7 L Niskin bottle to sample the upper 20 cm of the water column. These included 250 mL subsamples for $\text{CH}_4/\text{N}_2\text{O}$ analysis (bottles capped with butyl rubber stoppers and crimp-sealed), analysis of the CO_2 system (one bottle each for total CO_2 (C_T), total alkalinity (A_T), and pH) and 15 mL subsamples for the analysis of nutrients and DOC. Water for chlorophyll a determination was taken using 3 L canisters.

190 In the laboratory, $\text{CH}_4/\text{N}_2\text{O}$ and CO_2 samples were poisoned with 500 μL and 200 μL of saturated HgCl_2 , respectively, and stored in the dark at 4°C until analysis. Subsamples for nutrients and DOC were filtered in the field with pre-combusted (450°C for 4 h) 0.7 μm glass-fiber filters (GF/F, Whatman[®]) and stored at -20°C . Samples for chlorophyll a were filtered in the laboratory with non-combusted 0.7 μm glass-fiber filters (GF/F, Whatman[®]) and likewise stored at -20°C .

2.2.2 Chamber-based atmospheric GHG flux sampling for CO_2 and CH_4

195 Starting in June 2019, nearly 6 months before rewetting, GHG exchange was regularly measured using dynamic closed chambers (Livingston and Hutchinson, 1995) along a transect representing a soil humidity gradient (Figure 2b). The measurements were conducted twice a month, for a total of 11 sampling days at six peatland stations and two additional stations in the north-south-oriented main ditch. Each station was sampled up to eight times per sampling day, resulting in overall 418 CO_2 and 184 CH_4 pre-rewetting flux measurements.

200 For each measurement, the chambers were placed on permanently installed collars and connected through an airtight seal, with a closure period between 180 and 300 s. To ensure coverage of photosynthetic and respiration activity, CO_2 measurements were conducted using opaque and transparent chambers. To cover a broad spectrum of solar radiation, two additional measurements were conducted with cloth-covered transparent chambers, resulting in a reduced photosynthetically active photon flux density (PPFD). Changes in GHG concentrations in the chamber headspace were measured using a portable laser-based analyzer (Picarro G4301, GasScouter, Santa Clara, USA; LI-820, LI-COR Biosciences, Lincoln, USA and an Ultraportable Greenhouse Gas Analyzer (UGGA), Los Gatos Research Inc., Mountain View, Calif., USA).

After rewetting, the stations along the transect covered a gradient of ground elevations, including stations that fell dry at low water levels and stations that remained permanently flooded. Atmospheric GHG fluxes were measured twice a month using floating opaque chambers placed on the water surface above the same sampling locations of the flooded

Gelöscht: After rewetting, a

peatland. Since the flooding caused most plants to die, and almost all measurement locations were covered by water during the study period, we skipped the NEE measurements with transparent chambers. Approximately six measurements per station were made during 23 sampling days between December 2019 and December 2020, with a total of 698 CO₂ and 482 CH₄ fluxes determined during the post-rewetting year.

Gelöscht: Since transparent chambers were no longer used, PPFD variation was no longer considered.

215 2.3 Data processing, statistics, and definition of seasons and means

Data analysis and visualization were performed using R (R Core Team, 2020) and the packages *tidyverse* (Wickham et al., 2019), *lubridate* (Grolemund and Wickham, 2011), *patchwork* (Pedersen, 2020) *car* (Fox and Weisberg, 2019), and *flux* (Jurasinski et al., 2014). The relationships between environmental variables, nutrient concentrations, and GHG concentrations/fluxes were investigated in linear regression analyses. The significance level was set to $p < 0.05$.

220 To describe temporal patterns during the entire sampling period, we defined two pre- and four post-rewetting periods, roughly akin to seasons (Table 1). For a direct comparison between the pre- and post-rewetting periods, we compared nutrient and GHG flux data from summer and autumn 2019 with those from summer and autumn 2020 (Table 3) by using the Mann-Whitney-U test.▼

Gelöscht: For direct comparisons between pre- and post-rewetting, two pre-rewetting and four post-rewetting seasons were defined (Table 1).

Table 1. Defined seasons of the investigation period

	Pre-rewetting		Post-rewetting			
season	summer 2019	autumn 2019	winter 2019/2020	spring 2020	summer 2020	autumn 2020
months	June–August	September–November	December–February	March–May	June–August	September–December

225 We analyzed the data of the peatland and the inner bay stations, respectively, in order to verify the use of means for each sampling site and date. The difference between spatial (sampling stations) and temporal (sampling seasons) data variability was tested by using a Two-Way ANOVA and showed a higher temporal variability ($p < 0.05$). Therefore, we decided to combine the stations of the peatland and the inner bay, respectively, to report mean values and standard deviations (single values can be found in the published data set). The Two-Way ANOVA was also used to identify seasonal differences between the peatland and the inner bay (Table 2).

Gelöscht: The difference between spatial (sampling stations) and temporal (sampling seasons) data variability was tested and indicated a higher temporal variability.

230 At station D3, in the inner bay, the pH, CH₄, and pCO₂ values differed significantly from those of the remaining stations of the inner bay during the year after rewetting (ANOVA, Kruskal-Wallis test). Since the differences in water temperature, salinity, and O₂ were not significant, we decided to include the data from D3 for these variables to obtain a 235 larger data pool for the inner bay and to exclude D3 for all other variables.

2.4 Nutrients (NO_3^- , NO_2^- , NH_4^+ , PO_4^{3-}), chlorophyll a and DOC

245 2.4.1 Analysis

Nutrient analyses were carried out according to standard photometric methods (Grasshoff et al., 2009) by using a continuous segmented flow analyzer (SEAL Analytical QuAAstro, SEAL Analytical GmbH, Norderstedt, Germany). Detection limits were $0.2 \mu\text{mol L}^{-1}$ for NO_3^- , $0.05 \mu\text{mol L}^{-1}$ for NO_2^- , $0.5 \mu\text{mol L}^{-1}$ for NH_4^+ and $0.1 \mu\text{mol L}^{-1}$ for PO_4^{3-} . Measurements of the nutrient concentrations were partly below the detection limit for the peatland, the inner bay and the central bay (flagged in the published dataset). For example, for measurements below detection limit, it is recommended to use the actual values of these measurements (e.g. Fiedler et al., 2022) to achieve a robust statistical analysis. Since these data were not available, we decided to use randomly generated values between 0 and the respective detection limit with a uniform distribution for these measurements.

Chlorophyll a was extracted from glass-fiber filters (GF/F, Whatman[®]) by incubation with 96 % ethanol for 3 h and 255 afterwards analyzed by using a fluorometer (TURNER 10-AU-005, Turner Designs, San José, USA) at 670 nm after Edler (1979). DOC was analyzed after high-temperature combustion using a Multi 2100S instrument (Analytik Jena GmbH, Jena, Germany) and detected by non-dispersive infrared spectrometry after ISO 20236, ISO 8245 I, and EN 1484.

2.4.2 Use of reference data from a monitoring station

Coastal nutrient data (NO_3^- , NO_2^- , NH_4^+ and PO_4^{3-} concentrations) from a monitoring station in the Kubitzer Bodden 260 ("central bay", Figure 1b) ~15 km away from the study area were obtained as reference. Monitoring data from 2016 to 2020 were included. In detail, these data were used (1) to compare them with nutrient concentrations from the inner bay before and after rewetting to detect potentially higher concentrations, resulting from nutrient leaching within the peatland and a subsequent export into the inner bay and (2) to calculate the total possible export out of the peatland (Sect. 2.4.3) by using the monitoring station as a second, unaffected endmember besides the inner bay, which is by contrast potentially affected by 265 the rewetting. Due to transformations and potential losses along the way to the monitoring station, especially of the nitrogen species, the calculated total possible export has to be considered as maximum estimate.

2.4.3 Nutrient transport calculation (DIN-N and $\text{PO}_4\text{-P}$)

To calculate the bulk exchanges of dissolved inorganic nitrogen (DIN-N) and $\text{PO}_4\text{-P}$ between the flooded peatland and the inner bay/central bay, the water level was transformed to water volume by creating a hypsographic curve with increments of 270 0.1 m and a resolution of 1x1 m (Figure 3). Water level data from a nearby monitoring station ("Barhöft", 54.43°N , 13.03°E) and topography data with a resolution of 1x1 m were obtained from the Wasserstraßen- und Schifffahrtsamt Ostsee (WSA) and the Landesamt für innere Verwaltung MV, respectively. To ensure that the water level data of the monitoring station were valid for the peatland, the water level data of the latter, measured between August and December

2020, were compared with the data from the monitoring station, which showed a strong correlation ($r_s = 0.95, p < 0.001$, 15-275 min intervals, data not shown).

A water level of -1.6 masl, as the lowest recorded water level within the last 25 years, was used as the starting point to derive the cumulative water volumes of the peatland. The water volumes were then assigned to the corresponding water levels to finally calculate the water volume changes (Q , in $\text{m}^3 \text{ s}^{-1}$) according to Eq. (1):

$$Q(t) = \frac{dV}{dt} \quad (1)$$

where V is the water volume and t the time. Positive volume changes ($Q > 0$) indicate an inflow of water into the peatland 280 and vice versa. For each season, the mean inflow (Q_{in}) and outflow (Q_{out}) volumes were calculated according to Eqs. (2) and (3):

$$Q_{in} = \frac{1}{\Delta T} \int_t^{t+\Delta T} Q^{positive} dt \quad \text{for } Q > 0 \quad (2)$$

$$Q_{out} = \frac{1}{\Delta T} \int_t^{t+\Delta T} Q^{negative} dt \quad \text{for } Q < 0 \quad (3)$$

where ΔT denotes the season length. Note that Q_{out} is negative. [Seasonal mean values of nutrient concentrations \(DIN and PO₄³⁻\) were calculated and converted from \$\mu\text{mol L}^{-1}\$ to \$\text{kg m}^{-3}\$ by using the molecular masses of the basic elements N and P to derive DIN-N and PO₄-P.](#) After the conversion, nutrient masses of the peatland ($c_{peatland}$) and the inner bay (c_{IB}) vs. 285 peatland and central bay (c_{CB}), respectively, were multiplied by Q_{out} and Q_{in} and integrated to calculate the net nutrient transport (NNT, in tonnes) according to Eqs. (4) and (5):

$$NNT = \int_t^{t+\Delta T} Q_{in} c_{IB} dt + \int_t^{t+\Delta T} Q_{out} c_{peatland} dt \quad (4)$$

$$NNT = \int_t^{t+\Delta T} Q_{in} c_{CB} dt + \int_t^{t+\Delta T} Q_{out} c_{peatland} dt \quad (5)$$

Negative values indicate a net nutrient export from the peatland into the inner/central bay, and positive values display a net 290 nutrient import into the peatland. [Uncertainty ranges for the seasonal NNTs \(\$u_{NNT}\$, as 95 % confidence level\) were calculated as standard errors \(SE\) by using an error propagation according to Eq. \(6\):](#)

$$u_{NNT} = \sqrt{(c_{bay} dt u_{Qin})^2 + (c_{peat} dt u_{Qout})^2 + (Q_{out} dt u_{cpeat})^2 + (Q_{in} dt u_{cbay})^2} \quad (6)$$

where terms with "u" denote the respective SE as 95 % confidence level. To gain the annual SE of the NNT, all seasonal SE were added up.

Gelöscht: Nutrient concentrations (DIN and PO₄³⁻) were converted from $\mu\text{mol L}^{-1}$ to kg m^{-3} by using the molecular masses of the basic elements N and P to derive DIN-N and PO₄-P.

Gelöscht: –

Gelöscht: –

2.5 GHG concentrations and fluxes

2.5.1 Inorganic carbon system analysis

295 Directly measured variables (C_T, A_T, pH)

The inorganic carbon system was determined by analyzing the total CO_2 (C_T), total alkalinity (A_T), and pH of the water samples. C_T was measured with an automated infrared inorganic carbon analyzer (AIRICA, S/N #027, Marianda, Kiel, Germany). The system acidifies a discrete sample volume (phosphoric acid, 10 %), whereby the inorganic carbon species of C_T are shifted to $\text{CO}_{2\text{(g)}}$. A carrier gas stream (99.999 % N_2) transfers the gaseous components to a Peltier device and a 305 Nafion® drying tube (Perma Pure Nafion®, Ansyco GmbH, Karlsruhe, Germany) to remove water residues. The produced $\text{CO}_{2\text{(g)}}$ is detected by an infrared detector (LICOR 7000; LI-COR Environmental GmbH, Bad Homburg, Germany). Certified reference materials (CRM; Scripps Institution of Oceanography, University of California, San Diego, USA) were used for calibration. Triplicate measurements were conducted for each sample, and a precision of $\pm 5 \text{ }\mu\text{mol kg}^{-1}$ was achieved.

310 A_T was measured by potentiometric titration (glass electrode type LL Electrode plus 6.0262.100, Metrohm, Filderstadt, Germany) in the open-cell configuration, after Dickson et al. (2007). The system was calibrated with the same CRM as used for C_T and resulted in the same precision.

315 The pH was analyzed spectrophotometrically using the pH-sensitive indicator dye m-cresol purple (mCP, 2 mmol L^{-1} , Contros System and Solution GmbH, Kiel, Germany). The measurement principle and instrumental setup are described elsewhere (Dickson et al., 2007; Carter et al., 2013). In brief, absorption was measured using the Agilent 8453 UV-visible spectroscopy system (Agilent Technology, Waldbronn, Germany); pH parameterization for brackish water was calculated following Müller and Rehder (2018). Quality control was performed by measuring buffer solutions (salinity of 20) prepared according to Müller et al. (2018). An external buffer solution with a salinity of 35 (Scripps Institution of Oceanography, University of California, San Diego, USA) was additionally used. All pH values are reported given on the total scale (pH_T).

320 **Calculated variables**

The CO_2 partial pressure in the water phase (pCO_2), the value of which was required for the CO_2 air-water flux calculations (Sect. 2.5.3), was calculated from C_T and pH using the R packages *seacarb* (Gattuso et al., 2019), with K_1 and K_2 from Millero (2010), K_s from Dickson (1990), and K_f from Dickson and Riley (1979). C_T and pH were preferred because non-oceanic components, in particularly organic acid-base systems, contribute significantly to A_T (Kuliński et al., 2014). A_T was 325 also calculated from C_T and pH and the values compared with measured values, thus revealing the magnitude of the contributions of those components to A_T .

2.5.2 Dissolved CH_4 and N_2O concentration analysis

Dissolved CH_4 and N_2O concentrations were determined by gas chromatography on an Agilent 7890B instrument (Agilent Technologies, Santa Clara, USA) coupled to a flame ionization detector (FID) and an electron capture detector (ECD). A 330 purge and trap technique, explained in detail in Sabbaghzadeh et al. (2021) was used. In brief, a helium gas stream was used to purge 10 mL of seawater to extract volatile compounds. The gas stream passed through a purifier (VICI Valco Instruments Co. Inc., Houston, USA) and was dried using a Nafion® tube (Perma Pure Nafion®, Ansyco GmbH, Karlsruhe, Germany) and a SICAPENT® tube (Merck KGaA, Darmstadt, Germany). The relevant compounds were enriched by cryofocusing on a

trap filled with HayeSep D® (CS Chromatographie Service GmbH, Langerwehe, Germany) maintained at -120°C using an 335 ethanol/nitrogen cooling bath. After 10 minutes of heating in a 95°C water bath, the compounds were desorbed and separated by two capillary columns linked to the detectors by a Deans Switch (Pönisch, 2018).

For quality control, a calibration standard (gas composition: 9.9379 ppm CH₄ (± 0.0159 ppb) and 1982.07 ppm N₂O (± 3.77 ppb)) was measured daily before and after the sample measurements; the standard deviation was $< 1\%$. The 340 calibration range was adjusted using multi-loop injection of the calibration gas to ensure that the samples were within the limits of the calibration. The standard was recalibrated according to high-precision standards (ICOS-CAL laboratory, Max Planck Institute, Jena, Germany).

2.5.3 GHG flux calculations

Atmospheric fluxes based on closed-chamber measurements

CO₂ and CH₄ fluxes were calculated using the ideal gas law (Livingston and Hutchinson, 1995), as formulated in Eq. (7):

$$F = \frac{MpV}{RTA} * \frac{dc}{dt} \quad (7)$$

345 where F is the GHG flux ($\text{g m}^{-2} \text{ h}^{-1}$), M is the molar mass of the gas (g mol^{-1}), p is the standard air pressure (101,300 Pa), V is the chamber volume (m^3), R is the gas constant ($\text{m}^3 \text{ Pa K}^{-1} \text{ mol}^{-1}$), T is the temperature in the chamber (K), A is the surface area of the measurement collar (m^2), and dc/dt is the change in concentration over time. The latter was derived from the slope of a linear median-based regression. The atmospheric sign convention was applied; thus, positive fluxes indicated a release of GHG by the soil and negative fluxes GHG uptake by the soil. The fluxes were estimated using the function *fluxx()* 350 of the R package *flux* (Jurasinski et al., 2014) and the SLP method.

Atmospheric fluxes based on air-sea gas exchange parameterization (velocity k model)

The air-sea gas exchange (F, $\text{g m}^{-2} \text{ h}^{-1}$) is a function of the gas transfer velocity (k) and the concentration difference between the bulk liquid (C_w) and the top of the liquid boundary layer adjacent to the atmosphere (C_a). It was calculated as reported in Wanninkhof (2014) and as shown in Eq. (8):

$$F = k (C_w - C_a) \quad (8)$$

355 where k was derived from an empirical relationship between a coefficient of gas transfer (0.251) and the wind speed $\langle U^2 \rangle$ (Wanninkhof, 2014) and Schmidt number (Sc), as expressed by Eq. (9):

$$k = 0.251 \langle U^2 \rangle (Sc/660)^{(-0.5)} \quad (9)$$

Wind speeds originated from the nearby (~15 km away) monitoring station Putbus and were measured at 10 m height (DWD; 54.3643° N, 13.4771° E, WMO-ID 10093). The average wind speed was defined in this study ± 3 h from midday, because the wind speed over 24 h was lowest at night and highest at midday and because sampling was usually conducted 360 within the selected time interval. The Schmidt number was approximated by a linear interpolation between the freshwater and seawater values. Atmospheric-equilibrium conditions (C_a) were calculated using the atmospheric data for CO₂ and CH₄ obtained from the ICOS station “Utö” (Finnish Meteorological Institute, Helsinki). Due to the seasonal changes in the

atmospheric dry molar fraction of CO₂ and CH₄, mean values for each season were computed. For N₂O, the atmospheric dry mole fraction from station Mace Head was selected (National University of Ireland, Galway; data from the NOAA GML

365 carbon cycle cooperative global air sampling network (Dlugokencky et al., 2019a, 2019b)). A mean value of the atmospheric N₂O concentration during the investigation period was calculated due to its minor seasonality. Equilibrium concentrations were then calculated using the solubility coefficient (K₀) from Weiss and Price (1980). [We acknowledge that the air-sea exchange model we used](#) (Wanninkhof, 2014) [was developed for open ocean waters and is a doubtful approach for deriving fluxes in small enclosed areas such as our working area. However, the lack of an appropriate parameterization, and the](#)

370 [convincing result of the comparison of our two approaches \(see below and Appendix C\) justify our approach.](#)

Comparability of two independent approaches to atmospheric flux determination

We evaluated the comparability of the two previously described methods by comparing the results of a representative station (BTD7) for each post-rewetting season. The comparison showed no significant differences between the fluxes of CO₂ and CH₄ derived with the different methods and therefore, it seems appropriate to combine the fluxes for each GHG into one

375 pooled post-rewetting data set. The pooled post-rewetting flux values were compared with the pre-rewetting values to investigate the effect of rewetting on CH₄ and CO₂ fluxes (Table 3). For more details concerning the comparability assessment, see Appendix C. Due to the large variability and the pooling of chamber-based measurements with k model data, the GHG fluxes after rewetting are hardly suitable for upscaling and thus, the single values in the published data should be used.

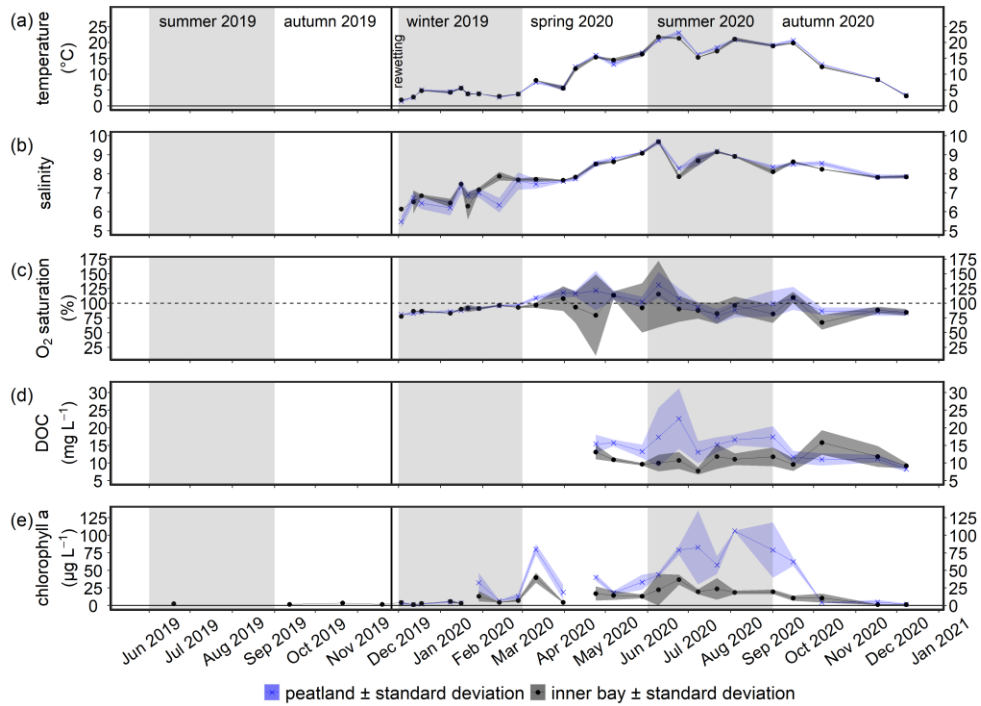
380 3. Results

3.1 Surface water properties (temperature, salinity, O₂, DOC, chlorophyll a)

In the first year after rewetting, there were no significant differences between the peatland and the inner bay with respect to surface water temperature, salinity and O₂ saturation (Figure 4a–c, Table 2), suggesting a pronounced water exchange between the peatland and the inner bay that was driven by frequent changes in the water level (Figure A1). [Additionally, no](#)

385 [significant differences between summer and autumn 2019 and summer and autumn 2020 were found in the inner bay.](#)

Temperature and salinity measurements near the peat surface showed no significant differences between the surface and bottom water over the year (n_{surface} = 140, n_{bottom} = 86, data not shown), which suggested that vertical exchange processes and mixing were highly pronounced. However, the significant difference in O₂ saturation between the surface and bottom water in summer ($p < 0.01$) indicated that local and temporary gradients are possible.



390

Figure 4. Time series of the mean (a) temperature, (b) salinity, (c) O₂ saturation, (d) DOC concentration and (e) chlorophyll a concentration (\pm standard deviations) in the surface water from June 2019 to December 2020. Data from the flooded peatland ($n=6$) are shown in blue and data from the inner bay ($n=2$ or 3, as explained in Sect. 2.3) in black. The vertical black line indicates the rewetting event.

395

DOC concentrations were significantly higher in the peatland than in the inner bay in spring and summer, with the highest concentration ($\sim 30 \text{ mg L}^{-1}$) measured in the peatland (Figure 4d, Table 2). Chlorophyll a concentrations after rewetting showed clear seasonal and spatial differences, with significantly higher concentrations in the peatland in spring and summer (max. $\sim 125 \text{ \mu g L}^{-1}$, Figure 4e, Table 2). A comparison of pre- and post-rewetting chlorophyll a concentrations in the inner bay in summer and autumn showed higher concentrations after rewetting (pre-rewetting: $2.5 \pm 0.9 \text{ \mu g L}^{-1}$, post-400 rewetting: $15.4 \pm 11.5 \text{ \mu g L}^{-1}$).

Table 2. Seasonal comparison of the surface water means (\pm standard deviation) in the peatland (“peat”) as opposed to the inner bay (“bay”) for all in situ variables. The number of observations is shown in parentheses, and significant seasonal differences ($p < 0.05$) between the inner bay and the peatland are indicated in bold.

		Pre-rewetting		Post-rewetting			
		summer 2019	autumn 2019	winter 2019	spring 2020	summer 2020	autumn 2020
temperature (°C)	peat	N/A	N/A	3.73 \pm 1.25 (45)	12.03 \pm 4.17 (35)	19.85 \pm 2.44 (30)	12.94 \pm 6.61 (30)
	bay	25.17 \pm 3.27 (3)	13.95 \pm 3.59 (6)	3.86 \pm 0.99 (17)	12.17 \pm 4.09 (17)	19.36 \pm 2.68 (15)	12.52 \pm 6.58 (15)
salinity	peat	N/A	N/A	6.67 \pm 0.68 (45)	8.23 \pm 0.66 (35)	8.96 \pm 0.50 (30)	8.22 \pm 0.33 (30)
	bay	9.21 \pm 0.69 (4)	8.39 \pm 0.38 (6)	6.99 \pm 0.65 (17)	8.27 \pm 0.56 (17)	8.86 \pm 0.63 (15)	8.13 \pm 0.32 (15)
O ₂ (mg L ⁻¹)	peat	N/A	N/A	11.19 \pm 0.74 (45)	11.72 \pm 1.93 (35)	8.60 \pm 1.86 (30)	9.34 \pm 1.35 (30)
	bay	7.66 \pm 1.70 (3)	7.48 \pm 3.87 (6)	11.18 \pm 0.67 (17)	10.03 \pm 3.48 (17)	8.26 \pm 2.26 (15)	8.86 \pm 1.80 (15)
chlorophyll a (μ g L ⁻¹)	peat	N/A	N/A	8.55 \pm 10.80 (24)	40.03 \pm 26.39 (12)	74.03 \pm 29.01 (10)	30.57 \pm 37.50 (10)
	bay	2.66 \pm N/A (1)	2.42 \pm 1.09 (3)	4.76 \pm 2.31 (8)	13.52 \pm 8.90 (8)	21.91 \pm 11.04 (10)	8.83 \pm 7.76 (10)
DOC (μ mol L ⁻¹)	peat	N/A	N/A	N/A	14.82 \pm 2.13 (18)	16.95 \pm 6.09 (27)	12.07 \pm 3.47 (29)
	bay	N/A	N/A	N/A	11.78 \pm 2.12 (6)	10.72 \pm 2.73 (10)	11.09 \pm 2.54 (10)
NO ₃ ⁻ (μ mol L ⁻¹)	peat	N/A	N/A	100.03 \pm 57.66 (45)	25.22 \pm 46.03 (35)	0.14 \pm 0.10 (29)	3.69 \pm 3.99 (30)
	bay	0.36 \pm 0.30 (4)	2.33 \pm 2.80 (6)	68.50 \pm 40.67 (9)	15.38 \pm 30.68 (11)	0.16 \pm 0.12 (10)	3.38 \pm 3.56 (10)
NO ₂ ⁻ (μ mol L ⁻¹)	peat	N/A	N/A	1.49 \pm 0.62 (45)	0.43 \pm 0.44 (35)	0.23 \pm 0.12 (29)	0.99 \pm 1.03 (30)
	bay	0.11 \pm 0.07 (4)	0.19 \pm 0.11 (6)	1.04 \pm 0.49 (9)	0.29 \pm 0.33 (11)	0.16 \pm 0.12 (10)	1.11 \pm 1.20 (10)
NH ₄ ⁺ (μ mol L ⁻¹)	peat	N/A	N/A	30.02 \pm 26.13 (45)	2.27 \pm 1.56 (35)	5.54 \pm 6.48 (29)	18.78 \pm 19.50 (30)
	bay	1.67 \pm 1.33 (3)	3.00 \pm 1.70 (6)	21.47 \pm 23.42 (9)	1.71 \pm 1.13 (11)	2.82 \pm 3.87 (10)	17.03 \pm 21.78 (10)
PO ₄ ³⁻ (μ mol L ⁻¹)	peat	N/A	N/A	0.37 \pm 0.41 (45)	0.26 \pm 0.28 (35)	0.49 \pm 0.26 (29)	0.35 \pm 0.33 (30)
	bay	1.30 \pm 1.90 (4)	0.12 \pm 0.08 (6)	0.21 \pm 0.21 (9)	0.09 \pm 0.13 (11)	0.22 \pm 0.21 (10)	0.26 \pm 0.28 (10)
CH ₄ (nmol L ⁻¹)	peat	N/A	N/A	47.96 \pm 49.52 (46)	300.49 \pm 414.29 (35)	1502.36 \pm 693.36 (30)	733.74 \pm 699.17 (30)
	bay	N/A	N/A	81.37 \pm 106.93 (7)	130.12 \pm 190.54 (11)	502.47 \pm 479.31 (10)	194.70 \pm 186.49 (20)
N ₂ O (nmol L ⁻¹)	peat	N/A	N/A	85.53 \pm 152.45 (46)	15.42 \pm 4.97 (35)	6.95 \pm 1.35 (30)	14.34 \pm 4.04 (30)
	bay	N/A	N/A	26.74 \pm 9.69 (7)	13.13 \pm 4.13 (11)	8.76 \pm 1.26 (10)	16.68 \pm 5.27 (10)
pCO ₂ (μ atm)	peat	N/A	N/A	1403.89 \pm 674.79 (46)	925.64 \pm 868.56 (35)	4016.69 \pm 2120.03 (30)	2197.11 \pm 1771.41 (30)
	bay	N/A	N/A	1050.00 \pm 552.68 (7)	297.81 \pm 93.57 (11)	1161.74 \pm 1275.46 (10)	1151.68 \pm 968.31 (10)
pH	peat	N/A	N/A	7.66 \pm 0.21 (46)	8.01 \pm 0.33 (35)	7.35 \pm 0.34 (30)	7.60 \pm 0.32 (30)
	bay	N/A	N/A	7.78 \pm 0.20 (7)	8.32 \pm 0.13 (11)	7.95 \pm 0.48 (10)	7.86 \pm 0.36 (10)
C _T (μ mol kg ⁻¹)	peat	N/A	N/A	2153.61 \pm 121.07 (46)	2471.11 \pm 223.74 (35)	2539.09 \pm 225.34 (30)	2273.41 \pm 312.95 (30)
	bay	N/A	N/A	2113.87 \pm 73.73 (7)	2201.63 \pm 98.45 (11)	2094.51 \pm 208.11 (10)	2106.76 \pm 282.17 (10)
A _T (μ mol kg ⁻¹)	peat	N/A	N/A	2154.43 \pm 155.12 (46)	2614.86 \pm 209.57 (35)	2546.03 \pm 239.96 (30)	2290.59 \pm 272.70 (30)
	bay	N/A	N/A	2144.41 \pm 94.49 (7)	2414.45 \pm 123.87 (11)	2270.25 \pm 125.07 (10)	2187.83 \pm 213.75 (10)

Gelöscht: Seasonal means (\pm standard deviation) of the surface water in the peatland (“peat”) and the inner bay (“bay”) for all in situ variables. The number of observations is shown in parentheses. *, ** and *** indicate $p < 0.05$, $p < 0.01$ and $p < 0.001$.

410 **Table 3.** Statistical comparison of pre- and post-rewetting nutrient concentrations and GHG fluxes. For pre- and post-rewetting phases, summer and autumn seasons were used (June to November 2019 and 2020, respectively). Nutrient concentrations are compared for the inner bay and GHG fluxes for the peatland site. *** and "n.s." indicate $p < 0.001$ and not significant, respectively.

location	Pre-rewetting		Post-rewetting		<i>p</i>	
	mean \pm SD	n	mean \pm SD	n		
NH_4^+ ($\mu\text{mol L}^{-1}$)	inner bay	2.6 \pm 1.6	9	9.9 \pm 16.9	20	n.s.
NO_3^- ($\mu\text{mol L}^{-1}$)	inner bay	1.5 \pm 2.3	10	1.8 \pm 2.9	20	n.s.
NO_2^- ($\mu\text{mol L}^{-1}$)	inner bay	0.2 \pm 0.1	10	0.6 \pm 1.0	20	n.s.
PO_4^{3-} ($\mu\text{mol L}^{-1}$)	inner bay	0.6 \pm 1.3	10	0.2 \pm 0.2	20	n.s.
CO_2 flux ($\text{g m}^{-2} \text{h}^{-1}$)	transect + area	0.3 \pm 0.8	330	0.3 \pm 0.3	450	n.s.
CO_2 flux ($\text{g m}^{-2} \text{h}^{-1}$)	ditch	0.3 \pm 0.1	87	0.3 \pm 0.3	92	n.s.
CH_4 flux ($\text{mg m}^{-2} \text{h}^{-1}$)	transect + area	0.1 \pm 1.0	97	1.7 \pm 7.6	320	***
CH_4 flux ($\text{mg m}^{-2} \text{h}^{-1}$)	ditch	11.4 \pm 37.5	85	8.5 \pm 26.9	92	***

3.2 Nutrients (NO_3^- , NO_2^- , NH_4^+ , PO_4^{3-})

3.2.1 Pre- and post-rewetting spatio-temporal dynamics and comparison with a nearby monitoring station

415 In the inner bay, all N-nutrient concentrations were substantially higher at the first sampling after rewetting than prior to rewetting, while PO_4^{3-} concentrations were only slightly higher post-rewetting (Figure 5). [This increase of N-nutrients led to a drastic increase of the N:P ratio from ~73 in autumn 2019 before rewetting to ~1600 shortly after rewetting in winter 2019](#). A comparison of the same pre- and post-rewetting seasons (summer and autumn 2019/2020) showed generally higher N-nutrient concentrations in the inner bay after rewetting [which could not be confirmed statistically \(Mann-Whitney-U-test, Table 3\)](#).

420 During winter, all N-nutrients were high in the peatland and inner bay. After a rapid decrease in spring, N-nutrient concentrations reached their lowest values during summer, with NH_4^+ and NO_2^- then increasing in autumn again. PO_4^{3-} concentrations followed a different pattern, with the highest concentrations determined in summer and fewer fluctuations over the year.

425 The spatial differences in nutrient [concentrations](#) between the inner bay and the peatland after rewetting [varied greatly between the nutrient species. From the N-nutrients, only \$\text{NO}_3^-\$ concentrations were significantly higher once in winter, shortly after rewetting, whereas \$\text{NH}_4^+\$ and \$\text{NO}_3^-\$ concentrations showed no significant differences in any season](#) (Table 2). Significantly higher PO_4^{3-} concentrations in the peatland occurred during [spring and summer \(\$p < 0.05\$ \)](#). [Some significant correlations between nutrient species were found \(Figure D1\), especially between \$\text{NO}_2^-/\text{NH}_4^+\$ and \$\text{NO}_3^-/\text{NO}_2^-\$ both in the peatland and the inner bay](#).

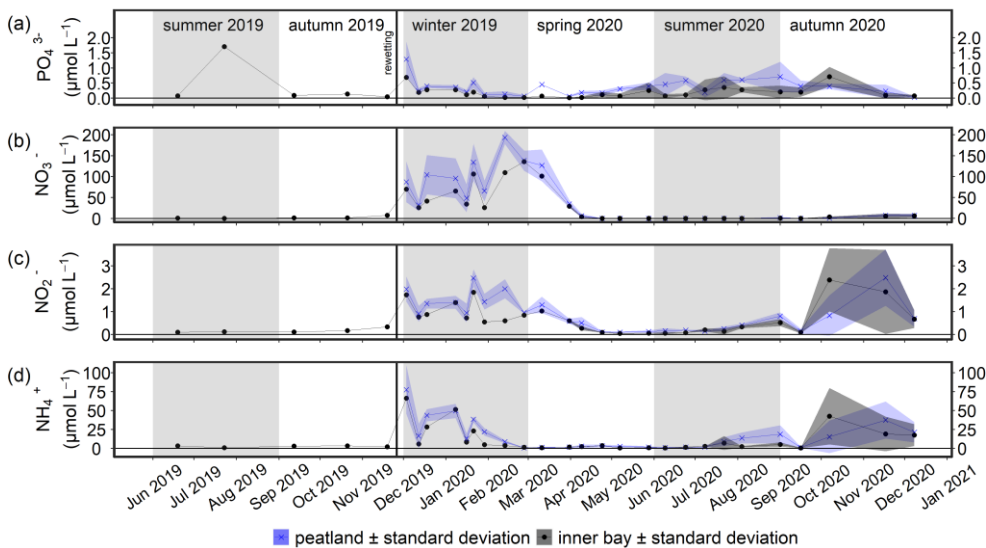
430 Nutrient concentrations of the monitoring station ("central bay") showed a low inter-annual variability during the years 2016-2020 and often lower concentrations than the inner bay (Figure 6). A detailed comparison of nutrient data from the monitoring station with those from the inner bay showed that before rewetting, only the NH_4^+ concentrations were

Gelöscht: However, as there were fewer measurements before rewetting, this finding could not be confirmed statistically.

Gelöscht: were significant only for NO_3^- concentrations, which were higher in the peatland ($p < 0.05$). The mean concentrations of NH_4^+ and NO_2^- were also generally, but not significantly, higher in the peatland than in the inner bay

440 significantly higher in the inner bay. After rewetting, NO_3^- and NO_2^- concentrations in the inner bay increased and were significantly higher than in the central bay ($p < 0.001$ and $p < 0.05$, respectively). In spring, N-nutrient concentrations were similar at the two locations whereas in summer, all N-nutrients were significantly higher in the inner bay ($p < 0.01$). In 445 autumn, NO_2^- and NH_4^+ concentrations increased again and thus, showed significantly higher concentrations in the inner bay. PO_4^{3-} again followed a pattern different from that of the N-nutrients. Shortly before rewetting, its concentrations in the inner bay were significantly lower than those in the central bay ($p < 0.05$). After rewetting, PO_4^{3-} concentrations showed no significant differences in any season.

Gelöschte: Compared to the monitoring station ("central bay", Sect. 2.4.2), only the NH_4^+ concentrations were significantly higher in the inner bay shortly before rewetting (Figure 6).



450 **Figure 5.** Time series of the mean (a) PO_4^{3-} , (b) NO_3^- , (c) NO_2^- , and (d) NH_4^+ concentrations (\pm standard deviations) in the surface water from June 2019 to December 2020. Data from the flooded peatland ($n = 6$) are shown in blue and data from the inner bay (until 11 March 2020: $n = 1$, thereafter: $n = 2$) in black. The vertical black line indicates the rewetting event.

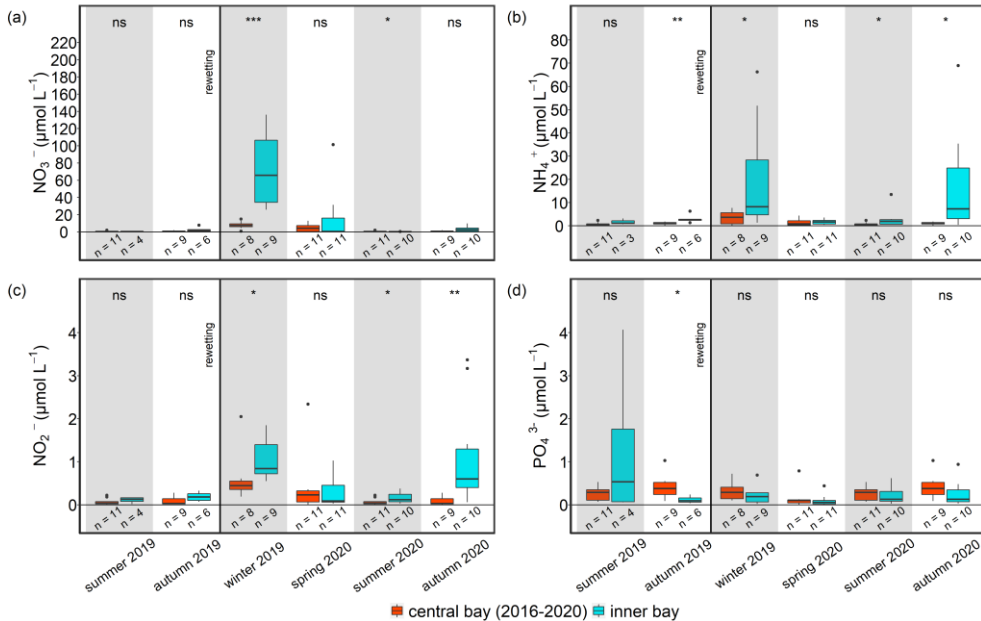


Figure 6. Seasonal nutrient concentrations of (a) NO_3^- , (b) NH_4^+ , (c) NO_2^- , and (d) PO_4^{3-} at the nearby monitoring station (central bay, red) and in the inner bay (inner bay, blue) from pre- to post-rewetting. The vertical black line indicates the rewetting event. Note that 5-year-data (2016–2020) are shown for the central bay (see Sect. 2.4.2). ns = not significant, * = $p < 0.05$, ** = $p < 0.01$, *** = $p < 0.001$.

3.2.2 Nutrient export from the rewetted peatland into the inner bay

The rewetted peatland was a net source of DIN-N and PO_4 -P for the inner bay (Table B1). During the first year after rewetting, $10.8 \pm 17.4 \text{ t yr}^{-1}$ DIN-N and $0.24 \pm 0.29 \text{ t yr}^{-1}$ PO_4 -P were exported into the inner bay. DIN-N export was highest during the winter directly after rewetting ($8.6 \pm 9.9 \text{ t}$) and lowest during summer ($0.3 \pm 0.5 \text{ t}$). DIN-N and PO_4 -P were only exported from the peatland into the inner bay in all seasons.

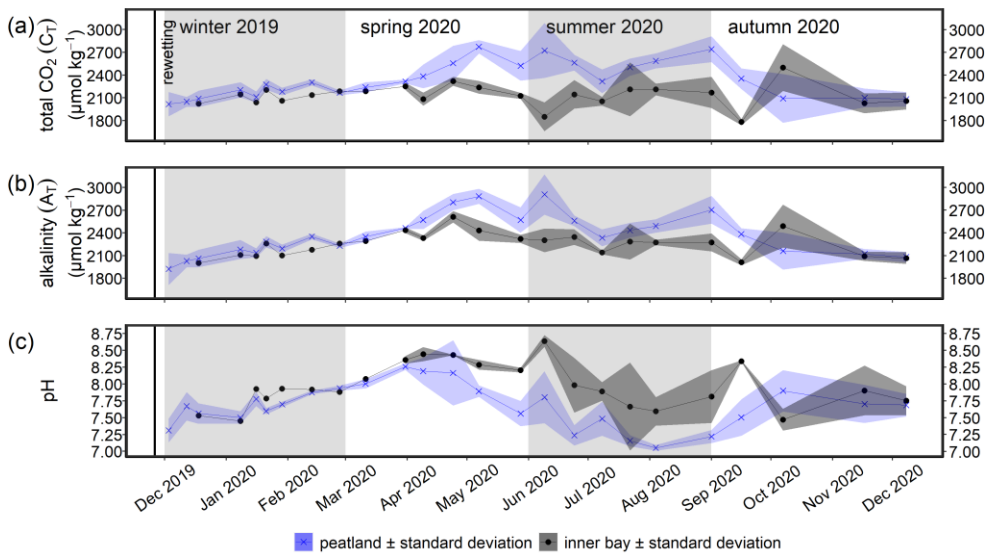
N-nutrient concentrations showed a gradient from the peatland through the inner bay to the central bay. Therefore, nutrient data from the central bay were also taken into account to estimate the total possible export from the peatland to the sea. This resulted in an estimated total net export of $33.8 \pm 9.6 \text{ t yr}^{-1}$ DIN-N. In contrast to the comparison of the peatland and the inner bay, PO_4 -P was once imported from the central bay into the peatland in autumn ($0.03 \pm 0.10 \text{ t}$). Additionally, it was noticeable that the PO_4 -P concentrations in the central bay were permanently higher than in the inner bay, leading to a lower annual export of $0.09 \pm 0.32 \text{ t yr}^{-1}$ PO_4 -P.

- Gelöscht:** 12.5
- Gelöscht:** 19.5
- Gelöscht:** 5
- Gelöscht:** 4
- Gelöscht:** , an import of PO_4 -P into the peatland occurred once in autumn.
- Gelöscht:** A gradient consisting mainly of N-nutrient concentrations occurred
- Gelöscht:** 36.5
- Gelöscht:** 10.9
- Gelöscht:** 2
- Gelöscht:** 3

3.3 GHG in the surface water after rewetting

3.3.1 Inorganic C system

During the winter after rewetting, the differences in the CO_2 system (C_T , A_T , pH, pCO_2) between the inner bay and the peatland were not significant (Figure 7, Figure 8a). All variables increased slightly until spring, coinciding with a slight increase in salinity over the same period. From spring onwards, however, the components of the CO_2 system followed contrasting patterns, with C_T and A_T remaining relatively constant in the inner bay but reaching significantly higher values in the peatland ($p < 0.05$), including maximum values in summer (Table 2). The pH also showed significant seasonal differences, with lower values and a minimum in summer in the peatland ($p < 0.05$). C_T and A_T values in the inner bay and in the peatland aligned in autumn whereas the pH remained significantly different ($p < 0.05$). The mean pCO_2 (calculated from C_T and pH) of the surface water in winter was $1050.0 \pm 55.7 \mu\text{atm}$ in the inner bay and $1403.9 \pm 674.8 \mu\text{atm}$ in the peatland (Figure 8a). The pCO_2 values were highest during the first few weeks after inundation and then steadily decreased, with the lowest mean values occurring in spring (peatland) and summer (inner bay). The summer was characterized by high pCO_2 values in general, including earlier and stronger increases in the peatland than in the inner bay that resulted in significant differences in spring and summer ($p < 0.05$ for both seasons). pCO_2 values were highest in summer with $4016.7 \pm 2120.0 \mu\text{atm}$ (peatland) and $1161.7 \pm 1275.5 \mu\text{atm}$ (inner bay) (Table 2). In October, all of the examined CO_2 quantities had a short-term inversion of the prevailing pattern.



500 **Figure 7.** Time series of the mean (a) total CO_2 (C_T), (b) total alkalinity (Ar), and (c) pH (\pm standard deviations) in the surface water after rewetting, as measured from December 2019 to December 2020. Data from the flooded peatland ($n = 6$) are shown in blue and data from the inner bay (until 11 March 2020: $n = 1$, thereafter: $n = 2$) in black. The vertical black line indicates the rewetting event.

3.3.2 CH_4

During the first few months after flooding (in winter), the CH_4 concentrations in both the inner bay and the peatland were low and did not differ significantly (Figure 8b, Table 2): $48.0 \pm 49.5 \text{ nmol L}^{-1}$ (peatland) and $81.4 \pm 107.0 \text{ nmol L}^{-1}$ (inner bay), respectively. From mid-spring onwards, CH_4 concentrations in the inner bay and the peatland increased such that during summer and autumn 2020, the differences at the two areas were significant ($p < 0.05$). Mean CH_4 values were highest in summer and amounted $1502.4 \pm 693.4 \text{ nmol L}^{-1}$ in the peatland and $502.5 \pm 479.3 \text{ nmol L}^{-1}$ in the inner bay. Further, the peatland was characterized by a considerable short-term variability in spring and summer, expressed in four peaks representing elevated concentrations. A positive significant correlation ($r_s = 0.73$, $n = 72$, $p < 0.001$) was found in the peatland between the surface water CH_4 concentrations and a water temperature $> 10^\circ\text{C}$, but not $< 10^\circ\text{C}$.

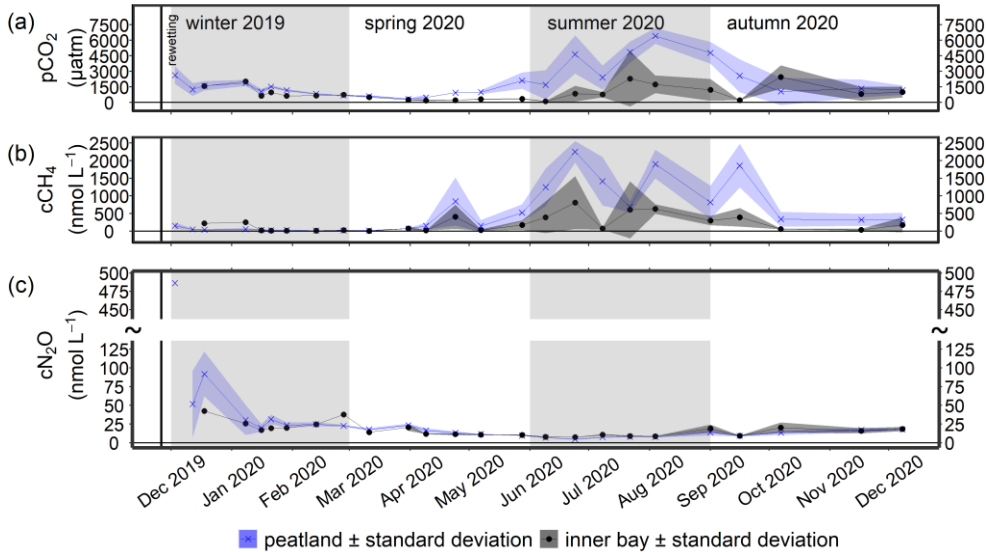


Figure 8. Time series of the mean (a) pCO_2 , (b) CH_4 concentration (cCH_4), and (c) N_2O concentration (cN_2O) (\pm standard deviations) after rewetting in the surface water from December 2019 to December 2020. Data from the flooded peatland ($n = 6$) are shown in blue and data from the inner bay (until 11 March 2020: $n = 1$, thereafter: $n = 2$) in black. The vertical black line indicates the rewetting event.

515 3.3.3 N₂O

The highest N₂O concentration of 486.3 nmol L⁻¹ was measured in the peatland one week after rewetting (Figure 8c), followed by 4–5 of still elevated N₂O concentrations between 19.9 and 91.8 nmol L⁻¹. During winter, significant positive correlations were determined in the peatland between N₂O and NH₄⁺ ($r_s = 0.61, n = 45, p < 0.001$) and between N₂O and NO₂⁻ ($r_s = 0.46, n = 45, p < 0.01$). From spring onwards, N₂O decreased rapidly, both in the peatland and the inner bay, with 520 the lowest values of 4.7 to 7.9 nmol L⁻¹ reached in summer. Other positive correlations of N₂O with N-nutrients in the peatland included NO₃⁻ ($r_s = 0.74, n = 35, p < 0.001$) and NO₂⁻ ($r_s = 0.70, n = 35, p < 0.001$) in spring and all N species in 525 autumn (NO₃⁻: $r_s = 0.85, n = 30, p < 0.001$; NO₂⁻: $r_s = 0.70, n = 30, p < 0.001$; NH₄⁺: $r_s = 0.80, n = 30, p < 0.001$).

Spatial differences in N₂O concentrations between the inner bay and the peatland were low and not significant in 530 winter, spring or autumn, whereas significantly lower concentrations were measured in the peatland during summer (Table 525 2).

3.4 Pre- and post-rewetting GHG fluxes (CO₂, CH₄, N₂O)

Terrestrial CO₂ fluxes before rewetting, during summer and autumn 2019, were highly variable ranging from -3.3 to 530 $3.0 \text{ g m}^{-2} \text{ h}^{-1}$ with a mean of $0.29 \pm 0.82 \text{ g m}^{-2} \text{ h}^{-1}$ (Figure 9a). Within the ditch, pre-rewetting CO₂ fluxes ranged from -0.008 to $0.6 \text{ g m}^{-2} \text{ h}^{-1}$, but on average were comparable to the fluxes determined at the terrestrial (dry) surface.

After rewetting, formerly terrestrial CO₂ fluxes decreased in amplitude (-0.5 to $1.4 \text{ g m}^{-2} \text{ h}^{-1}$), while the summer and autumn averages were unchanged compared to the pre-rewetting fluxes (Table 3). In the ditch, the mean and minimum post-rewetting CO₂ fluxes were within the range of those determined pre-rewetting (mean: $0.26 \pm 0.29 \text{ g m}^{-2} \text{ h}^{-1}$, min: 535 $-0.02 \text{ g m}^{-2} \text{ h}^{-1}$) but the maximum flux ($1.1 \text{ g m}^{-2} \text{ h}^{-1}$) was almost twice as high as the pre-rewetting ditch flux (max: $0.6 \text{ g m}^{-2} \text{ h}^{-1}$).

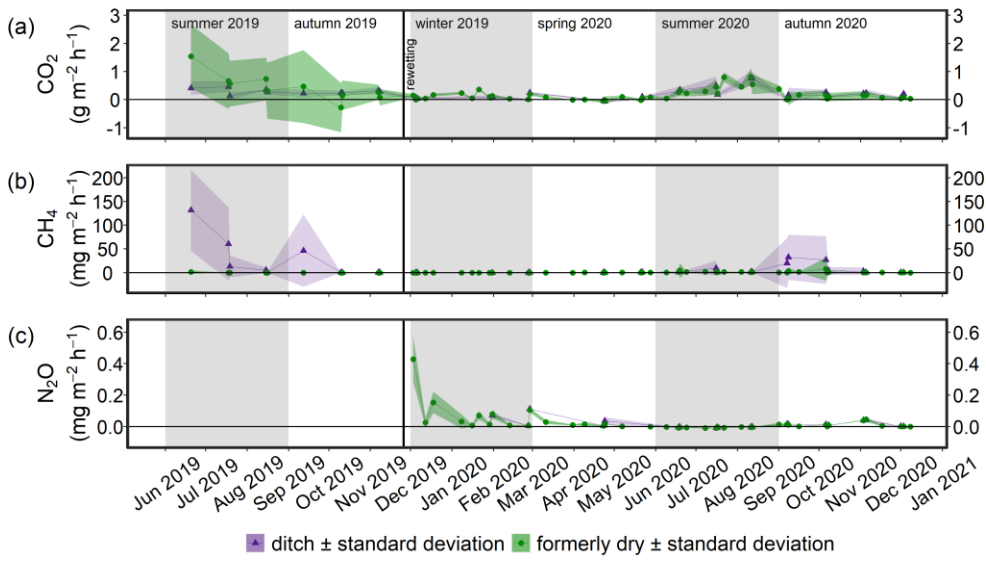
Pre-rewetting CH₄ fluxes in summer and autumn 2019 varied between -0.9 to $8.4 \text{ mg m}^{-2} \text{ h}^{-1}$ (terrestrial) and -1.1 to 540 $193.6 \text{ mg m}^{-2} \text{ h}^{-1}$ (drainage ditch; Figure 9b). While mean terrestrial CH₄ fluxes were $0.13 \pm 1.01 \text{ mg m}^{-2} \text{ h}^{-1}$, the mean ditch fluxes were $11.4 \pm 37.5 \text{ mg m}^{-2} \text{ h}^{-1}$. In summer and autumn 2020, after rewetting, average CH₄ fluxes on formerly terrestrial land increased slightly but significantly ($1.74 \pm 7.59 \text{ mg m}^{-2} \text{ h}^{-1}$), whereas in the ditch they decreased considerably (545 $8.5 \pm 26.9 \text{ mg m}^{-2} \text{ h}^{-1}$). Flux amplitudes at the ditch station before and after rewetting were comparable.

Data on N₂O fluxes are available only for the post-rewetting period. The rewetted peatland was a small source of N₂O, with an annual mean flux of $0.02 \pm 0.1 \text{ mg m}^{-2} \text{ h}^{-1}$ in the first year after rewetting (Figure 9c). The highest N₂O flux of 0.4 mg m⁻² h⁻¹ occurred one week after rewetting, followed by lower N₂O fluxes between 0.007 and 0.2 mg m⁻² h⁻¹ within the following 4–5 weeks. Afterwards, N₂O fluxes remained constantly close to zero. Negative fluxes, indicating N₂O uptake, 545 were measured only in summer.

Gelöscht: ~~Comparability of two independent approaches to atmospheric flux determination~~

Since the gas transfer velocity k model (Sect. 2.5.3) requires a water-air interface and thus cannot be applied to dry conditions, before rewetting only atmospheric flux measurements obtained by manual closed-chambers along a representative transect (Figure 2b) were available to determine pre-rewetting GHG fluxes. After rewetting, data from manual closed-chambers (transect) and from surface water sampling for the k model (transect and peatland stations) were used. The two methodologies were applied at the same locations along the transect only after rewetting (Table 3).¶

Table 3. Overview of the method usage to determine the atmospheric GHG fluxes¶
Pre-rewetting



560 **Figure 9.** Time series of the mean (a) CO_2 , (b) CH_4 , and (c) N_2O fluxes (\pm standard deviations) from June 2019 to December 2020. Fluxes of the permanently wet drainage ditch are shown in purple and those derived from the two methods employed in this study in green. The vertical black line indicates the rewetting event.

4. Discussion

565 4.1 Nutrient dynamics and export

The seasonal dynamics of the nutrients followed a typical course over the year. Thus, after rewetting, NH_4^+ , NO_3^- , and NO_2^- concentrations were high in winter and autumn, which is typically due to the mineralization of OM followed by nitrification (Voss et al., 2010). By contrast, the low DIN concentrations during spring and summer reflected the consumption of nutrients by plants and phytoplankton. The very high chlorophyll a concentration (up to $125 \mu\text{g L}^{-1}$) in the peatland indicated 570 the presence of a highly phototrophic community, likely driven by the higher availability of nutrients compared to the inner bay. Due to this distinct seasonal differences with the lowest nutrient concentrations in spring and summer, a rewetting within these seasons would probably be more beneficial to reduce a potential nutrient export into the inner bay, at least during the first few months after rewetting.

To assess whether the flooded peatland served as a nutrient source for the inner bay, nutrient concentrations of the 575 peatland were compared with those of the inner bay and of an unaffected monitoring station (“central bay”) and showed generally higher mean concentrations. Due to drainage, the mineralization of upper peat layers can lead to an accumulation

Gelöschte: Mean nutrient concentrations were generally higher in the peatland than in the inner bay but they increased in the latter after rewetting, suggesting rapid nutrient transport out of the peatland in the first 3 months (Figure 5). This was supported by significantly higher winter concentrations of all N-nutrients in the inner bay than in the central bay (Figure 6) whereas before rewetting, only the NH_4^+ concentration was significantly higher in the inner bay compared to the central bay. According to this result, the rewetting likely increased NO_3^- and NO_2^- concentrations in the inner bay due to a nutrient transport out of the peatland. ¶

of nutrients within the soil (Zak and Gelbrecht, 2007; Cabezas et al., 2012). After rewetting, nutrient concentrations in the porewater and ultimately in the overlying water increase (van de Riet et al., 2013; Harpenslager et al., 2015; Zak et al., 2017). The leaching of nutrients is driven by concentration differences across the soil-water interface, but it is also dependent 590 on factors such as salinity (Rysgaard et al., 1999; Steinmuller and Chambers, 2018), the oxygen availability in the soil (Lennartz and Liu, 2019), and the effects of the latter on microbial processes (Burgin and Groffman, 2012), as well as on the degree of peat decomposition (Cabezas et al., 2012). For instance, highly degraded peat, such as at our study area, can store and release more nutrients than less degraded peat (Cabezas et al., 2012), meaning that the highly degraded peat of our study 595 area was prone to leach high amounts of nutrients. Occasional measurements of porewater nutrient concentrations in the peat of your study area revealed DIN and PO_4^{3-} concentrations up to 1 order of magnitude higher than those in the surface water (Anne Breznikar, unpublished data), providing further support for the leaching of nutrients out of the peatland and into the inner bay.

The estimated annual nutrient exports from the peatland of $10.8 \pm 17.4 \text{ t yr}^{-1}$ DIN-N and $0.24 \pm 0.29 \text{ t yr}^{-1}$ $\text{PO}_4\text{-P}$ (peatland/inner bay) and $33.8 \pm 9.6 \text{ t yr}^{-1}$ DIN-N and $0.09 \pm 0.32 \text{ t yr}^{-1}$ $\text{PO}_4\text{-P}$ (peatland/central bay) were high, given the 600 small size of the flooded peatland ($\sim 0.5 \text{ km}^2$ at 0 masl). For comparison, the Warnow, a small river that flows into the Baltic Sea near the city of Rostock, Mecklenburg-Vorpommern, draining an area of $\sim 3300 \text{ km}^2$, had a mean annual DIN-N and $\text{PO}_4\text{-P}$ export of $1200 \pm 500 \text{ t yr}^{-1}$ and $19.9 \pm 7.6 \text{ t yr}^{-1}$, respectively, over the last 25 years (HELCOM, 2019). Therefore, the total nutrient export from the flooded peatland to the inner bay and to the central bay in the first year after rewetting accounted for ~ 1 and $\sim 3\%$, respectively, of the annual DIN-N and $\text{PO}_4\text{-P}$ loads of the Warnow. When normalized to the 605 same dimensions, our study area exported $21.6 \pm 7.6 \text{ t DIN-N km}^{-2} \text{ yr}^{-1}$ and $0.18 \pm 0.48 \text{ t } \text{PO}_4\text{-P km}^{-2} \text{ yr}^{-1}$, whereas the Warnow exported only $0.36 \text{ t DIN-N km}^{-2} \text{ yr}^{-1}$ and $0.01 \text{ t } \text{PO}_4\text{-P km}^{-2} \text{ yr}^{-1}$.▲

However, we also want to shortly address the reasons for the high uncertainty range of our calculated nutrient exports. Firstly, they derive from high fluctuating nutrient concentrations in the surface water within the seasons. This is also visible in the high standard deviations (Table 2). Therefore, the 95 % confidence level of the nutrient exports is high and reflects the natural dynamic. Secondly, we conducted default error propagation during the export calculation which leads to even higher ranges on top of the high natural dynamic.

Compared to the Warnow river, it is noticeable that the range of uncertainties is highly different for the two sources. While our uncertainties are mostly higher and in the same order of magnitude compared to the means, the uncertainties of the river data are one order of magnitude lower. This is likely due to the different time scales of the two data sets. Our export data were generated by taking only the first post-rewetting year into account in which the system was still in a transition state and thus, showed very dynamic nutrient concentrations. The uncertainties of the river exports were generated by using 25 years of data, leading to lower uncertainties than using data from only one year and they were calculated as standard deviation and not as standard error, as was done for the exports of our study site. Therefore, this has to be considered when their uncertainty ranges are compared directly. Nevertheless, our results highlight the importance of currently still

Gelöscht: 12.5

Gelöscht: 19.5

Gelöscht: 5

Gelöscht: 6

Gelöscht: 5

Gelöscht: 10.9

Gelöscht: 2

[1] verschoben (Einfügung)

Gelöscht: 25.0

Gelöscht: 73.0

Gelöscht: 4

[1] nach oben verschoben: Overall, the total nutrient export from the flooded peatland to the inner bay and to the central bay in the first year after rewetting accounted for ~ 1 and $\sim 3\%$, respectively, of the annual DIN-N and $\text{PO}_4\text{-P}$ loads of the Warnow.

[2] nach unten verschoben: These results highlight the importance of currently still unmonitored and small, independently draining areas along the coastline of the Baltic Sea, in particular those that become intentionally flooded (HELCOM, 2019).

[2] verschoben (Einfügung)

unmonitored and small, independently draining areas along the coastline of the Baltic Sea, in particular those that become intentionally flooded (HELCOM, 2019).

640 **4.2 Assessment of the GHG dynamics**

4.2.1 **CO₂**

The carbon system in our study area is governed by a variety of processes (e.g. Wolf-Gladrow et al., 2007; Kuliński et al., 2017; Schneider and Müller, 2018). C_T and A_T were transported with the brackish water from the central bay and ultimately from the Arkona Basin. Additional alkalinity can be added either by a supply of freshwater, which in the southwestern Baltic

645 Sea is characterized by higher alkalinities than the brackish or even saltwater endmember (Beldowski et al., 2010; Müller et al., 2016), or can be introduced by mineralization processes from the seafloor [in the inner bay and the flooded peatland](#). Primary production (i.e., carbon fixation) will decrease C_T, lower the pCO₂ and increase pH during the formation of organic matter. The mineralization of OM from various sources (new primary production, mineralization of the inundated former vegetation and from the underlying peat) will enhance C_T and A_T concentrations, increase pCO₂ and decrease pH. Air-sea 650 exchange during our study is fostered by a pCO₂ that is above atmospheric levels throughout the year, except for a short period in spring in the inner bay and the peatland, where outgassing of CO₂ occurred, resulting in lower pCO₂ and a decrease in C_T.

We observed three main developments in the surface water CO₂ system and air-sea flux pattern: (i) in winter 2019/2020, the CO₂ system hardly differed between the peatland and the inner bay; (ii) from spring to autumn, there were 655 significant differences in the CO₂ system between the peatland and the inner bay, with higher pCO₂, C_T and A_T values and lower pH in the peatland coinciding with an enrichment in chlorophyll a; (iii) overall, the first post-rewetting year showed sustained high, but less variable CO₂ fluxes compared to pre-rewetting conditions. In the following, we will discuss these three observations and set them into context.

(i) Initial post-rewetting CO₂ dynamics

660 The first weeks after the rewetting were characterized by high nutrient concentrations, a continuous increase in A_T, C_T and pH and a decrease in pCO₂ (Figure 5, Figure 7, Figure 8). The increase in C_T and A_T coincided with a steady increase in salinity (Figure 4), which is in line with a general increase of A_T with increasing salinity known for the western Baltic Sea (e.g. Kuliński et al., 2022).

665 Still, the A_T values at the given salinity were higher in the inner bay and the peatland than would be expected from a linear A_T/salinity relation found for surface waters in the open Baltic Sea from the central Gotland Sea to the Kattegat (Beldowski et al., 2010; Müller et al., 2016). Thus, the high A_T in the inner bay and peatland were likely associated with local carbonate (CaCO₃) weathering from terrestrial sources and/or a transport by groundwater (Schneider and Müller, 2018). C_T and A_T values during this period were consistently higher by ~70–80 μmol kg⁻¹ in the peatland than in the inner bay, consistent with enhanced leaching from the recently inundated peat. [Besides, local CaCO₃ weathering as well as local](#)

670 anoxic processes, such as SO_4^{2-} reduction may have increased the A_T in the submerged soil and finally contributed to higher A_T values compared to the inner bay.

The oversaturation in pCO_2 and potentially the excess leaching of alkalinity from the soil might have contributed to the decrease in pCO_2 and increase in pH in the peatland in winter 2019/2020. This was apparently reinforced by a short episode of primary production mid/end January, indicated by a steeper decline of the pCO_2 and a steeper pH increase. This 675 coincided with a short increase in chlorophyll a ($\sim 30 \mu\text{g L}^{-1}$) and a slight intermittent increase of the surface water temperatures (Figure 4). This short, unusually early productive period might have resulted from the high nutrient availability induced by the rewetting of the peatland (Sect. 3.2.1), in particular the high NH_4^+ levels, which simultaneously showed a sharp intermittent minimum.

(ii) Production and mineralization governance over the productive period (spring to autumn)

680 In late winter and the first half of spring, pCO_2 continuously decreased in the peatland as well as in the inner bay. Lowest pCO_2 was measured between March and May and coincided with enhanced chlorophyll a concentrations and a high availability of nutrients in the peatland and in the inner bay, which decreased until mid spring. This resulted in a slight CO_2 uptake in the peatland of $\sim -0.005 \text{ g m}^{-2} \text{ h}^{-1}$ for a short period of time, so that spring was the only season when pCO_2 was on 685 average below atmospheric concentrations in the inner bay (Figure 9). This finding can be attributed to the onset of the productive period, at still moderate surface water temperatures below 10°C until mid April. During this period, productivity clearly dominated mineralization, as suggested by the decreasing pCO_2 and increasing pH, despite rising temperatures, as well as increasing O_2 oversaturation in the surface waters. These trends were slightly more pronounced in the peatland than in the inner bay, in accordance to higher nutrient concentrations available for production.

690 From mid spring until late summer, the peatland was characterized by increased pCO_2 and a variable CO_2 system together with high mean chlorophyll a concentrations of up to $106.0 \mu\text{g L}^{-1}$. N-nutrients were very low and the system was clearly nitrogen-limited, with only slightly elevated NH_4^+ concentrations in late summer (Figure 4, Figure 5). Furthermore, the O_2 saturation shifted from over- to undersaturated conditions. These observations suggest that the peatland and the inner bay were characterized by simultaneous production and mineralization processes from mid spring until autumn that kept the N-nutrients (except PO_4^{3-}) low. Mineralization of OM in the water column, sediment and soil clearly dominated over 695 production, leading to the observed high pCO_2 , lowered pH, and enhanced A_T and C_T concentrations. Mineralization during this period was clearly more pronounced in the peatland than in the inner bay, leading to the higher pCO_2 , A_T , and C_T values in the peatland, and a stronger and more pronounced reduction of the pH. This stronger mineralization, in particular in the warm summer months, also led to higher DOC concentrations in summer, with a maximum in June/July coinciding with maximum surface water temperatures. The enhanced mineralization in the peatland was likely fueled by higher OM 700 availability from high decomposition rates of fresh plant substrate from inundated plant residuals (Glatzel et al., 2008; Hahn-Schöfl et al., 2011), and also due to the omission of topsoil removal before the rewetting. In addition, aerobic and anaerobic oxidation of CH_4 , that was produced in anoxic zones, might have led to increased CO_2 production, especially during increased water temperatures (e.g. Treude et al., 2005; Dean et al., 2018), due to the availability of SO_4^{2-} and O_2 .

Gelöscht: It is noteworthy that in the first spring after rewetting, there were negligible stands of emergent macrophytes, and the peatland area appeared like a shallow bay. The primary production can therefore be attributed to the water column.

The calculated A_T (from C_T and pH) in the peatland was consistently lower than the measured A_T with a difference in the range of $55\text{--}122 \mu\text{mol kg}^{-1}$ and thus of 2.7–4.7 % (data not shown). This difference was higher than in the Baltic Sea, 710 where the contribution of organic A_T is estimated to be 1.5–3.5% (Kuliński et al., 2014). Due to closer vicinity to the coast and the high amount of degradable OM, this higher contribution of organic A_T was to be expected. The highest discrepancy between measured A_T values and those calculated from pH and C_T occur in early summer, simultaneously to the highest values in DOC, in particular in the peatland (Figure 4). This suggests that the organic A_T related to the occurrence of DOC (and thus DOM), contributed to the excess of A_T . The higher DOC formation in summer in the peatland might partly explain 715 the difference in A_T between the inner bay and the peatland.

(iii) Sustained high CO_2 fluxes but less variability caused by brackish water flooding

The amplitude of the CO_2 fluxes from formerly drained parts of the study area decreased after rewetting with brackish water, while the amplitude of CO_2 fluxes from the ditch (inundated after flooding but with deeper, probably incompletely exchanged water) did not differ strongly before and after rewetting (Figure 9). An increased water table is the main driver for 720 the reduction of CO_2 emissions on formerly drained locations. A similar scenario has been reported for terrestrial sites (Bubier et al., 2003; Strack, 2008). In a nearby coastal peatland, both photosynthesis and ecosystem respiration were strongly reduced after rewetting (Koebisch et al., 2013). The rewetting of our study area probably caused a die-back of the highly productive grassland vegetation at a rate faster than that occurring after freshwater rewetting (Hahn-Schöfl et al., 2011), which in turn would have led to a reduction of the CO_2 flux amplitude.

725 Average summer/autumn CO_2 fluxes after rewetting had a mean of $0.26 \pm 0.29 \text{ g m}^{-2} \text{ h}^{-1}$ and remained thus relatively high compared with those fluxes from 2019. They were also higher than the fluxes determined in studies of shallow coastal or near-shore waters in the northwestern Bornholm Sea of up to $0.01 \text{ g m}^{-2} \text{ h}^{-1}$ (Thomas and Schneider, 1999) or the Bothnian Bay of around $\sim 0.0007 \text{ g m}^{-2} \text{ h}^{-1}$ (Löffler et al., 2012). In a nearby coastal fen recently influenced by brackish water inflow, ecosystem respiration was 2 orders of magnitude lower (Koebisch et al., 2020) compared to our study 730 site, where the ongoing decomposition of submerged substrate from plant residuals and the fresh soil may have fueled the continuously high CO_2 fluxes in the first year after rewetting (Hahn-Schöfl et al., 2011). The mineralization of OM from primary production driven by the high initial nutrient availability, as well as aerobic and anaerobic oxidation (Dean et al., 2018) of easily degradable substrates or CH_4 , might have additionally contributed to these CO_2 fluxes. We expect that CO_2 emissions will further decrease, likely because substrates become exhausted and a novel ecosystem will be established 735 (Kreyling et al., 2021), with developing algae fostering CO_2 fixation.

4.2.2 CH_4

We observed three main developments in surface water methane concentrations and flux patterns: (i) a short-term, very moderate increase in CH_4 concentrations directly after rewetting in winter 2019/2020; (ii) an increase in the CH_4 concentrations mainly from spring to autumn, that was significantly higher and more variable in the peatland than in the

740 inner bay and correlated with water temperature; (iii) in the first year after rewetting, much lower CH₄ fluxes than reported for nearby peatlands rewetted by freshwater. These three observations are discussed and set into context in the following.

(i) Short-term, moderate increase in the CH₄ concentrations in the winter after rewetting

The measurements in winter, immediately after rewetting, showed a short-term increase in the CH₄ concentrations, although remaining low (Figure 8). Rewetting with brackish water inundated both the degraded peat and the remaining vegetation. 745 While this implies the instant availability of labile OM, the intensity of methanogenesis depends not only on the total amount but also on the quality of the OM (Heyer and Berger, 2000; Parish, 2008). Inundated plant material and its subsequent die-back provide high-quality OM, so that in our study the availability of OM was not a limiting factor. Nevertheless, the CH₄ concentration remained low and was associated with low temperature, which is an important factor controlling microbial processes and CH₄ production. A study in a nearby shallow coastal area of the Baltic Sea, between the islands of Rügen and 750 Hiddensee, showed that water temperature was the primary driver of the temporal variability in CH₄ emissions, with low rates associated with low temperatures (Heyer and Berger, 2000).

The rewetting with brackish water transported water with a salinity of 6–7.4 into the peatland such that there were no significant differences in salinity compared to the inner bay in winter (same as for temperature; Table 2). Thus, sulfate reached the peatland immediately after rewetting. As a terminal electron acceptor (TEA), SO₄²⁻ promotes the establishment 755 of sulfate-reducing bacteria (SRB), which outcompete methane-producing microorganisms (methanogens) for substrates (Segers and Kengen, 1998; Jørgensen, 2006; Segarra et al., 2013). This process was shown to play an important role in flat brackish water systems (e.g. Heyer and Berger, 2000). The availability of other TEAs, such as NO₃⁻ that had high concentrations in our study of $\sim 100 \pm 58 \mu\text{mol L}^{-1}$, could have further suppressed methanogenesis (Table 2) (Jørgensen, 2006). Beside competitive mineralization, aerobic and anaerobic CH₄ oxidation may have reduced the CH₄ concentrations 760 (Heyer and Berger, 2000; Reeburgh, 2007; Knittel and Boetius, 2009; Steinle et al., 2017), supported by the effective exchange of water masses. Overall, the rewetting with brackish water during the cold winter season apparently inhibited methanogenesis and/or effective oxidation, resulting in low CH₄ concentrations and a small CH₄ flux into the atmosphere.

(ii) Increased and variable CH₄ concentrations during the vegetation period

The increasing temperature from spring to autumn was accompanied by an enhanced and albeit variable CH₄ concentrations. 765 Temperature is crucial in controlling CH₄ cycling in shallow coastal/near-shore waters as well as in wetlands, and a distinct relationship between temperature and CH₄ concentrations has been reported for brackish shallow water systems (Bange et al., 1998; Heyer and Berger, 2000) and for the organic-rich sediments in the North Sea (e.g. Borges et al., 2018). Similar relationships describe the CH₄ exchange in permanently inundated wetlands (e.g. Koelsch et al., 2015) and in a peatland close to our study site during the first year after rewetting (Hahn et al., 2015). Moreover, CH₄ concentrations in the peatland 770 ($r_s = 0.75$, $n = 74$, $p < 0.05$) and the inner bay ($r_s = 0.55$, $n = 29$, $p < 0.05$) correlated significantly and positively with temperature. In the study of Heyer and Berger (2000) the temperature range influenced the temporal variability in CH₄ emissions, which were highest in late spring. Since the temperature range in the peatland of our study was variable (e.g.,

maximum difference of ~ 6 °C between samplings), with the highest values between spring and autumn (7.4–23.1 °C), this variability may have contributed to the observed CH₄ dynamics.

775 The peatland and the inner bay were clearly influenced by the same hydrographic conditions, evidenced by their very similar salinities and temperatures. However, the peatland showed higher CH₄ concentrations from spring to late autumn, likely due to the high availability of OM as described by Heyer and Berger (2000) and Bange et al. (1998). Incubation experiments of a degraded fen grassland demonstrated the accumulation of fresh plant litter in a new sediment layer after flooding that resulted in high rates of CH₄ and CO₂ production (Hahn-Schöfl et al., 2011). A further potential 780 driver of OM availability is the sedimentation of freshly produced OM originating from primary production, as described for shallow areas in the Baltic Sea (Bange et al., 1998) and for a shallow bight in the North Sea, which in the latter led to a yearly peak in the seasonal CH₄ cycle (Borges et al., 2018). Although our observations were not made in OM-poor sediments, an impact of primary production on enhanced CH₄ concentrations in the OM-rich Drammendorf peatland is likely, given the significant positive correlation of the surface CH₄ concentrations and the chlorophyll a concentration 785 ($r_s = 0.41$, $n = 56$, $p < 0.05$). Furthermore, aerobic CH₄ production cannot be excluded, as its occurrence has been reported in oxic freshwater (Bogard et al., 2014) and during NO₃[−] limitation and PO₄^{3−} availability (Damm et al., 2010), conditions that also prevailed in spring and summer at our study site.

(iii) Brackish water rewetting and low CH₄ emissions

790 Despite high surface water CH₄ concentrations in the peatland and their inter-seasonal and spatial variability, rewetting with brackish water resulted in CH₄ emissions considerably lower than those from temperate fens rewetted with freshwater, where CH₄ emissions strongly increased (Augustin and Chojnicki, 2008; Couwenberg et al., 2011; Hahn et al., 2015; Franz et al., 2016; Jurasinski et al., 2016).

795 At our study site, although average CH₄ fluxes on formerly terrestrial locations increased significantly by 1 order of magnitude after rewetting, the overall increase from 0.13 ± 1.01 to 1.74 ± 7.59 mg m^{−2} h^{−1} (Figure 9) was lower than that reported for freshwater rewetted fens under similar climatological boundary conditions (e.g. Hahn et al., 2015; Franz et al., 2016). Even several years after rewetting, the annual CH₄ budgets of a shallow lake on a formerly drained fen varied between 4.0 and 91.0 g m^{−2} yr^{−1} (Franz et al., 2016), corresponding to 11.0–249.3 mg m^{−2} h^{−1}. Our CH₄ fluxes were also lower than the emissions reported from coastal-near shallow waters of the Baltic Sea, where fluxes of 39.9–104.2 mg m^{−2} h^{−1} were measured in June/July (Heyer and Berger, 2000). For the same months, mean CH₄ fluxes at the formerly dry stations in 800 our study site were 0.5–4.9 mg m^{−2} h^{−1}. However, compared to CH₄ fluxes from continental shelves (0.015–0.024 mg m^{−2} h^{−1}; adapted from Bange et al., (1994)), the fluxes of our study site were 2 orders of magnitude higher. Despite low average fluxes, emission peaks could be distinguished with the highest flux from the now inundated ditch of 149.2 mg m^{−2} h^{−1} in September 2020 and 108.3 mg m^{−2} h^{−1} in October 2020. While these values were still lower than the maximum value of 243.0 mg m^{−2} h^{−1} reported by Heyer and Berger (2000), it is important to stress that our study site was a 805 source of CH₄ already in its drained state, especially within the drainage ditch, where CH₄ fluxes were comparable to the ~ 0.2 mg m^{−2} h^{−1} reported from undrained fens (Danevčič et al., 2010).

The lower CH₄ emissions of the brackish rewetted Drammendorf peatland can be attributed to the availability of TEAs, especially SO₄²⁻, which (1) may have contributed to a suppression in methanogenesis by competitive inhibition (Segers and Kengen, 1998; Jørgensen, 2006; Segarra et al., 2013) or (2) fostered the anaerobic oxidation of methane (AOM) 810 as an effective pathway to reduce CH₄ emissions, and by (3) fast aerobic CH₄ oxidation mediated by oxygen-rich water. Significant CH₄ production rates in marine and brackish water settings have been reported only where SO₄²⁻ is depleted, such as in the porewater of an inundated and degraded fen (Hahn-Schöfl et al., 2011) or below the SO₄²⁻ penetration zone in marine settings (e.g. Boetius et al., 2000; Reeburgh, 2007). At our study site, the depth of SO₄²⁻ penetration was probably low due to the short impact of the brackish water. Moreover, AOM is sensitive to the introduction of O₂ mediated by wind- 815 driven resuspension (Treude et al., 2005). Since our study area was shallow and likely experiences regular wind-driven resuspension, spatially and temporally dynamic AOM can be assumed. However, the CH₄ fluxes suggested that an effective aerobic and anaerobic oxidation of CH₄ was more likely. Moreover, higher CH₄ concentrations in the peatland compared to the inner bay in combination with the high lateral water exchange due to frequent changes in the water level (Figure 3) should have driven a net advective export of CH₄-enriched water to the inner bay. This would have further contributed to the 820 low peatland CH₄ emissions and the observed high variability.

While CH₄ production and emission were likely prevented by rewetting with oxygen-rich, sulfate-containing brackish water, the possibility remains that the total CH₄ release was underestimated by unsufficient accounting for ebullition. In the marine environment, bubble-mediated transport is attributed to gassy sediments and an effective mechanism of vertical CH₄ migration (e.g. Borges et al., 2016). Although neither of the methods used to determine CH₄ 825 fluxes specifically account for ebullition, we estimated that 6.9 % of all analyzed chamber-based fluxes were partly bubble-influenced. We observed further that in another 9.6 % of the chamber-based flux measurements the CH₄ concentration patterns indicated ebullition, but these were not accounted for in the final calculations of diffusive flux. Thus, given that only 16.5 % of the chamber-based flux measurements indicated bubble-mediated CH₄ transport and in almost half of those cases, the resulting perturbation was small and was included in the flux amplitude, the magnitude of the ebullition-driven 830 underestimation of our flux estimates is considered to be small.

In summary, the increase in CH₄ concentrations after rewetting in winter was small, short-lived and associated with the die-back of plants. CH₄ fluxes in the first year after rewetting remained relatively low and were lower than typical for post-rewetting conditions. They also followed a seasonal pattern common for shallow organic-rich systems, with a strong correlation with temperature in spring and summer. The ongoing depletion of OM after the initial post-rewetting shock and a 835 new start of the ecosystem will likely lead to a decrease in CH₄ emissions.

4.2.3 N₂O

The rewetted peatland was a source of N₂O in the first year after rewetting, although the mean annual N₂O flux of 0.02 ± 0.07 mg m⁻² h⁻¹ was very low (Figure 9). This was expected since permanent inundation leads to anoxic conditions in the peat, preventing the production of N₂O (e.g. Succow and Joosten, 2001; Strack, 2008). However, the range of post-rewetting

840 N₂O fluxes in the first 3 months (winter) was clearly much larger than during the rest of the year, which indicated that N₂O was strongly and immediately affected by the rewetting, as shown elsewhere (Goldberg et al., 2010; Jørgensen and Elberling, 2012). The highest N₂O flux (0.4 mg m⁻² h⁻¹) and the highest NH₄⁺ concentration (78.0 µmol L⁻¹) was measured one week after rewetting and a significant positive correlation between these two variables was found in winter. Additionally, correlations of NO₂⁻/NH₄⁺ and NO₃⁻/NO₂⁻ were found in the peatland and in the inner bay (Figure D1). These 845 results suggested that N₂O was produced as a side product of nitrification, either in the surface water or in the peat. The accumulation of N₂O, but also of NO₂⁻ and NO₃⁻ in winter can be interpreted as a result from shifting O₂ conditions in the freshly inundated ecosystem, such that incomplete process chains of e.g. nitrification and denitrification were favored (Rassamee et al., 2011).

850 During late spring and early summer, undersaturation of the surface water with N₂O, compared to the atmosphere, pointed to consumption within suboxic/anoxic zones of the peat. Consumption in the surface water was unlikely because anoxic conditions were never found near the peat surface. The undersaturation of N₂O a few months after rewetting evidenced the change in O₂ conditions in the peat, from oxic to hypoxic/anoxic, turning the rewetted peatland into an N₂O sink, at least temporarily. This change was likely driven by the higher availability of fresh OM (measured as chlorophyll a) in the peatland compared to the inner bay, finally leading to significantly lower N₂O concentrations in the peatland in 855 summer ($p < 0.001$, Table 2).

860 Previously reported N₂O fluxes in drained peatlands range from 0.002 to 0.45 mg m⁻² h⁻¹, with a clear trend towards higher fluxes in fertilized or naturally N-rich areas (Flessa et al., 1998; Glatzel and Stahr, 2001; Augustin, 2003; Strack, 2008; Minkkinen et al., 2020). Augustin et al. (1998) examined multiple degraded fens in Mecklenburg-Vorpommern and Brandenburg (Germany) and calculated N₂O fluxes of 0.04 to 0.10 mg m⁻² h⁻¹ in extensively and intensively used fen grasslands, respectively (Augustin et al., 1998). N₂O fluxes in drained peatlands result from low water level which allows the penetration of oxygen into the peat to fuel N₂O producing processes (Martikainen et al., 1993; Regina et al., 1999). As the water level in our study site was permanently below the soil surface before rewetting, it is likely that it was a source of N₂O. The mean post-rewetting N₂O flux determined in our study area (0.02 ± 0.07 mg m⁻² h⁻¹) is in the lower range of fluxes from drained peatlands. Therefore, as shown in other studies (Succow and Joosten, 2001; Minkkinen et al., 2020), the rewetting 865 very likely led to a reduction of N₂O fluxes.

870 In general, the N₂O fluxes in rewetted peatlands are in the same range as fluxes from pristine ones (Minkkinen et al., 2020), indicating that rewetting is a very effective measure to reduce N₂O emissions to natural levels. Literature values range from up to 0.01 and 0.02 mg m⁻² h⁻¹ for rewetted and undrained boreal peatlands (Minkkinen et al., 2020), respectively, to 0.08 mg m⁻² h⁻¹ for a rewetted riparian wetland near a freshwater meadow (Kandel et al., 2019). Although it is difficult to compare the N₂O fluxes determined in this study to those of other sites with different salinities, hydrologies and also histories of usage, our mean annual post-rewetting value lies in the lower range of N₂O fluxes previously reported for rewetted and pristine peatlands.

Gelöscht: Additionally, there was a significant positive correlation between these two variables in winter.

875 5. Conclusions

The effects of rewetting a drained coastal peatland with brackish water in winter and the subsequent formation of a permanently inundated area were studied over one year.

We found a strong pulse of DIN leaching out of the peat followed by the transport of DIN into the inner bay, leading to a high export especially in winter compared to the Warnow, a nearby river. However, due to a rapid decrease of 880 nutrient concentrations in spring, the nutrient export after a rewetting in spring or summer would likely be lower compared to rewetting in winter, at least during the first few months thereafter.

Further, CO₂ concentrations and emissions seem to remain relatively high after the rewetting with brackish water compared to the dry conditions before rewetting. This was likely driven by the high OM availability from the residual vegetation but also by the high rate of primary production in the water column. However, the flux amplitude decreased after 885 rewetting and thus, peak emissions during the vegetation period were prevented. The lack of a strong increase of CH₄ emissions in the first year after rewetting with brackish water, in contrast to nearby areas rewetted with freshwater, suggests that especially during the colder months, rewetting with brackish water or seawater would minimize CH₄ emissions and thus maximize the effect on integrated GHG emission reduction. Moreover, a rapid elevation of the water level, as occurred at our 890 study site, will promote the oxidation of peat-derived CH₄ in the water column. Future CH₄ emissions will depend on processes, such as the development of vegetation and will likely decrease. According to literature, it is likely that the peatland was a rather large source of N₂O before rewetting due to its drainage for agricultural use. However, the permanent inundation initialized a rapid decrease of N₂O emissions and converted the peatland into a N₂O sink during summer, with fluxes similar to pristine peatlands.

With the ongoing formation of salt grass meadows, livestock farming at our study area can and will continue. 895 However, the area's use has not hindered its positive development towards an ecosystem with the potential to eventually become a carbon and nutrient sink in the future. We expect that both the nutrient export and GHG emissions will slowly decrease due to a shrinking reservoir of substrates. Nonetheless, because degraded peat is both nutrient- and OM-enriched, this decrease will occur slowly, given that the topsoil was not removed prior to flooding to diminish nutrients and OM, as 900 was demonstrated by other studies. [Whether or not the area will act as a C sink in the future depends on the success and speed of the establishment of vascular vegetation and its burial in the anoxic parts of the sediment.](#)

Nutrient export from peatlands and the re-establishment of the nutrient and C-sequestration functions of highly degraded coastal peatlands after rewetting are complex processes whose elucidation requires long-term investigations. The pronounced seasonal dynamics highlight the need for approaches that include a high temporal resolution, such as achieved with sensor-based or eddy-supported measurements.

905 **Appendix A: Study area**

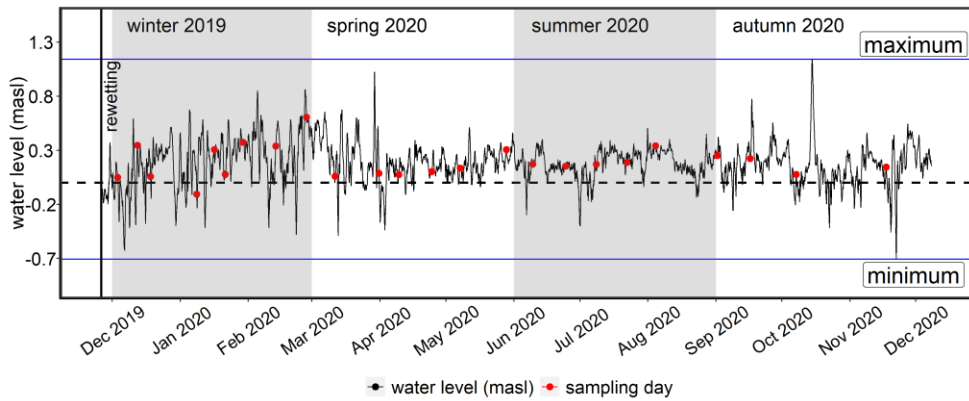


Figure A1. Water level data from the monitoring station “Barhöft” (WSA Ostsee), representing the Kubitzer Bodden, from the beginning of rewetting (26 November 2019) until the end of the investigation period. The red dots indicate the sampling days. The dashed horizontal line represents 0 masl. The minimum and maximum water levels of the investigation period are shown by the blue horizontal lines (~0.7 masl and 1.1 masl, respectively). See also Figure 3 and Figure A2.

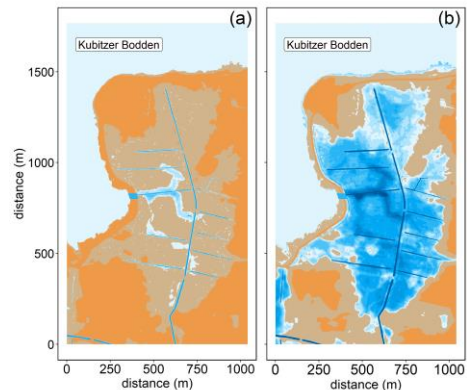


Figure A2. The changing water level and its effect on the water coverage of the study area, shown for (a) -0.5 masl and (b) 0.5 masl. Topography data retrieved from AfGVK, LAiV MV.

Appendix B: Nutrient export calculation

915 **Table B1.** Seasonal water volume exchanges (Q_{in}/Q_{out} , $m^3 s^{-1}$) and nutrient masses ($kg m^{-3}$) \pm standard error in the inner bay (c_{IB}), the central bay (c_{CB}), the peatland ($c_{peatland}$), and the resulting net nutrient transport (NNT, in tonnes) for DIN-N and PO_4 -P. Negative values of NNT indicate an export from the peatland into the inner bay/central bay and *vice versa*.

season	Q_{in} ($m^3 s^{-1}$)	Q_{out} ($m^3 s^{-1}$)	c_{IB} $DIN-N$ ($kg m^{-3}$)	$c_{peatland}$ $DIN-N$ ($kg m^{-3}$)	NNT $DIN-N$ (t)	c_{IB} PO_4 -P ($kg m^{-3}$)	$c_{peatland}$ PO_4 -P ($kg m^{-3}$)	NNT PO_4 -P (t)
winter	1.9 ± 0.1	-1.9 ± 0.1	1270×10^{-6} $\pm 506 \times 10^{-6}$	1840×10^{-6} $\pm 267 \times 10^{-6}$	-8.6 ± 9.9	6.5×10^{-6} $\pm 5.0 \times 10^{-6}$	11.5×10^{-6} $\pm 3.7 \times 10^{-6}$	-0.08 ± 0.10
spring	1.3 ± 0.1	-1.3 ± 0.1	243×10^{-6} $\pm 289 \times 10^{-6}$	391×10^{-6} $\pm 220 \times 10^{-6}$	-1.5 ± 3.8	2.8×10^{-6} $\pm 2.8 \times 10^{-6}$	8.1×10^{-6} $\pm 3.1 \times 10^{-6}$	-0.05 ± 0.04
summer	1.1 ± 0.1	-1.1 ± 0.1	44.0×10^{-6} $\pm 38.2 \times 10^{-6}$	82.7×10^{-6} $\pm 34.6 \times 10^{-6}$	-0.3 ± 0.5	6.8×10^{-6} $\pm 4.7 \times 10^{-6}$	15.2×10^{-6} $\pm 3.1 \times 10^{-6}$	-0.07 ± 0.05
autumn	1.2 ± 0.1	-1.2 ± 0.1	301×10^{-6} $\pm 218 \times 10^{-6}$	328×10^{-6} $\pm 104 \times 10^{-6}$	-0.4 ± 3.2	8.1×10^{-6} $\pm 6.2 \times 10^{-6}$	10.9×10^{-6} $\pm 3.7 \times 10^{-6}$	-0.04 ± 0.10
total (peatland / inner bay)				-10.8 ± 17.4				-0.24 ± 0.29
season	Q_{in} ($m^3 s^{-1}$)	Q_{out} ($m^3 s^{-1}$)	c_{CB} $DIN-N$ ($kg m^{-3}$)	$c_{peatland}$ $DIN-N$ ($kg m^{-3}$)	NNT $DIN-N$ (t)	c_{CB} PO_4 -P ($kg m^{-3}$)	$c_{peatland}$ PO_4 -P ($kg m^{-3}$)	NNT PO_4 -P (t)
winter	1.9 ± 0.1	-1.9 ± 0.1	169×10^{-6} $\pm 63.1 \times 10^{-6}$	1840×10^{-6} $\pm 267 \times 10^{-6}$	-26.2 ± 5.4	9.9×10^{-6} $\pm 5.9 \times 10^{-6}$	11.5×10^{-6} $\pm 3.7 \times 10^{-6}$	-0.02 ± 0.11
spring	1.3 ± 0.1	-1.3 ± 0.1	85.1×10^{-6} $\pm 42.1 \times 10^{-6}$	391×10^{-6} $\pm 220 \times 10^{-6}$	-3.1 ± 2.4	4.3×10^{-6} $\pm 4.7 \times 10^{-6}$	8.1×10^{-6} $\pm 3.1 \times 10^{-6}$	-0.04 ± 0.06
summer	1.1 ± 0.1	-1.1 ± 0.1	20.2×10^{-6} $\pm 9.5 \times 10^{-6}$	82.7×10^{-6} $\pm 34.6 \times 10^{-6}$	-0.5 ± 0.3	8.4×10^{-6} $\pm 3.4 \times 10^{-6}$	15.2×10^{-6} $\pm 3.1 \times 10^{-6}$	-0.06 ± 0.04
autumn	1.2 ± 0.1	-1.2 ± 0.1	26.5×10^{-6} $\pm 9.1 \times 10^{-6}$	328×10^{-6} $\pm 104 \times 10^{-6}$	-3.9 ± 1.5	13.0×10^{-6} $\pm 6.5 \times 10^{-6}$	10.9×10^{-6} $\pm 3.7 \times 10^{-6}$	0.03 ± 0.10
total (peatland / central bay)				-33.8 ± 9.6				-0.09 ± 0.32

Appendix C: Comparability of two independent approaches to atmospheric flux determination

920 Since the gas transfer velocity k model (Sect. 2.5.3) requires a water-air interface and thus cannot be applied to dry conditions, atmospheric flux measurements obtained by manual closed-chambers along a representative transect (Figure 2b) were available to determine pre-rewetting GHG fluxes (CO_2 and CH_4). After rewetting, data from manual closed-chambers (transect) and from surface water sampling for the k model (transect and peatland stations) were used. The two methodologies were applied at the same locations along the transect only after rewetting (Table C1).

925 **Table C1.** Overview of the methods used to determine the atmospheric GHG fluxes

Pre-rewetting	Post-rewetting	
transect (Figure 2b)	transect (Figure 2b)	peatland area (Figure 2a)
chamber-based	chamber-based ^{1,2}	k model ²

k model^{1,2}

¹ inter-methodological comparison at station BTD7

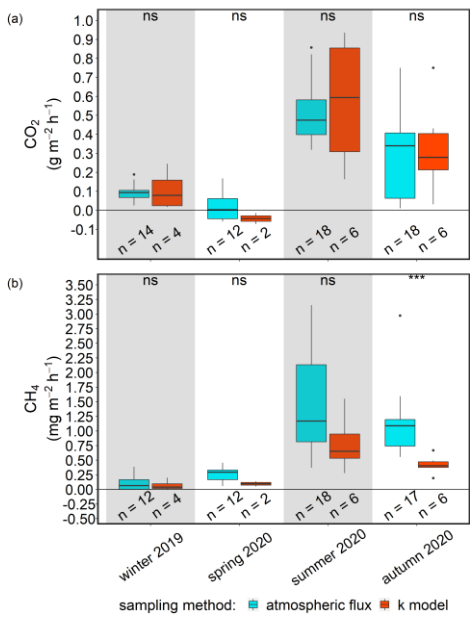
² formed the data representing post-rewetting fluxes

To evaluate the inter-comparability of the flux estimates obtained with the two methods, the results from station BTD7 were compared for each post-rewetting season (Figure C1). Data from this station were chosen because it was permanently flooded after rewetting and thus assured a valid baseline for comparison. The dynamics of the CO₂ fluxes determined by the

930 two methods were the same and thus did not differ significantly in any of the seasons (Kruskal-Wallis test, $p > 0.05$).

CH₄ fluxes also did not differ significantly, except in autumn (Kruskal-Wallis test, $p < 0.001$), when the average flux calculated according to the two methods differed by a factor of 2.7. However, the data of the k model had less impact, due to the smaller number of measurements ($n = 6$). Given the smaller data set compared to that of the closed chambers ($n = 17$), the same statistical analysis was conducted without a seasonal division. The results showed no significant 935 differences in the two methods for CH₄ fluxes (Kruskal-Wallis test, CO₂ and CH₄). Therefore, it was deemed appropriate to combine the flux-estimation methods for each GHG into one post-rewetting data set, as this allowed the consideration of a broader range of possible flux amplitudes. In addition, the post-rewetting data acquired along the transect were pooled with data distributed throughout the peatland area. Although the area covered by the transect was smaller than the covered by the k-model data from the peatland, such that pooling of the post-rewetting-data risked spatial bias, two positive effects of 940 pooling were identified: (1) The transect stations were representative of the entire area after flooding, because they covered a water-level-gradient (several cm to > 2 m in the ditch) that coincided with the conditions of the peatland stations. (2) The transect stations represented a large heterogeneity in the peatland before rewetting that decreased post-rewetting. This was also evident from the CO₂ flux measurements, which showed a high variability (data not shown) at each station before 945 rewetting. After rewetting, there was less variability such that the stations became more similar in their atmospheric C-exchange patterns, likely due to the mixing patterns triggered by lateral exchange with the Baltic Sea (Sect. 3.1). Largely similar conditions were therefore assumed at all stations within the peatland.

The pooled post-rewetting flux values were compared with the pre-rewetting values to investigate the direct effect of rewetting on CH₄ and CO₂ fluxes.



950 **Figure C1.** Seasonal post-rewetting fluxes of (a) CO_2 and (b) CH_4 at station BTD7 which is part of the GHG flux transect. Chamber-based atmospheric GHG fluxes are shown in blue and air-sea GHG fluxes from the k model in red. The methodological comparisons within seasons are based on a significance level of $p < 0.05$. ns: not significant; *** $p < 0.001$.

Appendix D: Nutrient cross plots

Cross plots with linear regression analyses were generated for nutrients (NH_4^+ , NO_3^- , NO_2^- , PO_4^{3-}) and DOC concentrations across all seasons to investigate potential correlations (Figure D1). Significant correlations are shown with red asterisks ($p < 0.05$).

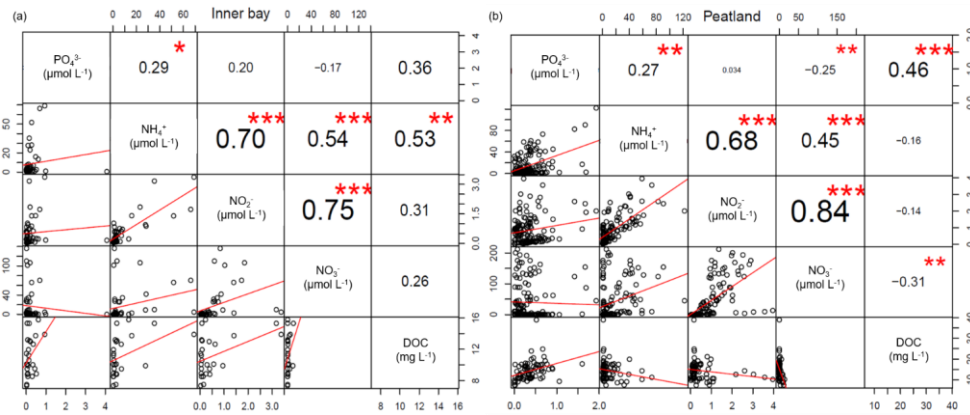


Figure D1. Cross plots of the measured nutrient (NH_4^+ , NO_3^- , NO_2^- , PO_4^{3-}) and DOC concentrations in (a) the inner bay and (b) the peatland across all seasons. Significant correlations are indicated by asterisks.

960

Data availability. The raw data used in this study are archived at <http://doi.io-warnemuende.de/10.12754/data-2022-0003>. The calculated GHG emission data used in this study are archived at <http://doi.io-warnemuende.de/10.12754/data-2022-0004>.

965 *Author contributions.* All authors designed the concept of the study. DLP, AB and CNG conducted the field work, data analysis, and interpretation. [DLP and AB wrote the first draft of the manuscript.](#) DLP created the figures and organized the data. AB conducted the statistical analysis. CNG wrote sections of the manuscript. All authors contributed to manuscript revision and approved the submitted version.

970 *Competing interests.* The authors declare that they have no conflict of interest.

Acknowledgements. The authors would like to thank Cindy Hoppe and Henning Sack for their great support during the field work; Lara Prelle, Petra Mutinova and the Biologische Station Zingst (all University of Rostock) for providing and measuring some additional nutrient data; Christian Burmeister, Dr. Stefan Otto (both IOW) and Dr. Stefan Köhler 975 (University of Rostock) for their technical laboratory assistance; Dr. Joachim Dippner, Dr. Marvin Lorenz and Dr. Christiane Hassenrück (all IOW) for their help on the nutrient export calculation and statistical analyses, respectively. Dr. Bita Sabbaghzadeh and Dr. Oliver Schmale (both IOW) provided valuable feedback on the manuscript. We are grateful to the Ostseestiftung and especially to Rasmus Klöpper, who guided the cooperation required for the project and provided valuable

data on the study area. We thank Sascha Klatt for information on the study area and especially for technical support during
980 field work. We also thank the Wasserstraßen- und Schifffahrtsamt Ostsee (WSA Ostsee) for water level data, the Landesamt
für innere Verwaltung Mecklenburg-Vorpommern (LAiV MV), Fachbereich Geodatenbereitstellung for topography data, the
Landesamt für Umwelt, Naturschutz und Geologie Mecklenburg-Vorpommern (LUNG MV), especially Mario von Weber,
for nutrient monitoring data and the DWD for meteorological data.

985 *Financial support.* This study was supported by the German Research Foundation (DFG) within the PhD graduate school
"Baltic TRANSCOAST" GRK 2000/1. A. Breznikar was funded by a doctoral scholarship from the Deutsche
Bundesstiftung Umwelt (DBU).

References

Augustin, J. (Ed.): Gaseous emissions from constructed wetlands and (re)flooded meadows, in: International Conference:
990 Constructed and Riverine Wetlands for Optimal Control of Wastewater at Catchment Scale, edited by: Mander, Ü., Vohla,
C. and Poom, A., Tartu Univ. Press, 2003.

Augustin, J. and Chojnicki, B.: Austausch von klimarelevanten Spurengasen, Klimawirkung und Kohlenstoffdynamik in den
ersten Jahren nach Wiedervernässung von degradiertem Niedermoorgrünland, Berichte des Leibniz-Institut für
Gewässerökologie und Binnenfischerei, 50–61, 2008.

995 Augustin, J., Merbach, W., Steffens, L., and Snelinski, B.: Nitrous Oxide Fluxes Of Disturbed Minerotrophic Peatlands,
Agribiological research (Germany), 51, 47–57, 1998.

Bange, H. W., Bartell, U. H., Rapsomanikis, S., and Andreae, M. O.: Methane in the Baltic and North Seas and a
reassessment of the marine emissions of methane, Global Biogeochem. Cycles, 8, 465–480,
<https://doi.org/10.1029/94GB02181>, 1994.

1000 Bange, H. W., Dahlke, S., Ramesh, R., Meyer-Reil, L.-A., Rapsomanikis, S., and Andreae, M. O.: Seasonal Study of
Methane and Nitrous Oxide in the Coastal Waters of the Southern Baltic Sea, Estuarine, Coastal and Shelf Science, 47, 807–
817, <https://doi.org/10.1006/ecss.1998.0397>, 1998.

Bartlett, K. B., Bartlett, D. S., Harriss, R. C., and Sebacher, D. I.: Methane emissions along a salt marsh salinity gradient,
Biogeochemistry, 4, 183–202, <https://doi.org/10.1007/BF02187365>, 1987.

1005 Beldowski, J., Löffler, A., Schneider, B., and Joensuu, L.: Distribution and biogeochemical control of total CO₂ and total
alkalinity in the Baltic Sea, Journal of Marine Systems, 81, 252–259, <https://doi.org/10.1016/j.jmarsys.2009.12.020>, 2010.

Bockholt, R.: Flächen-, Ertrags- und Problemanalyse des Überschwemmungsgrünlandes der Ostsee-, Bodden- und
Haffgewässer, Forschungsbericht Universität Rostock, 17, 1985.

Boetius, A., Ravenschlag, K., Schubert, C. J., Rickert, D., Widdel, F., Gieseke, A., Amann, R., Jørgensen, B. B., Witte, U.,
1010 and Pfannkuche, O.: A marine microbial consortium apparently mediating anaerobic oxidation of methane, *Nature*, 407,
623–626, <https://doi.org/10.1038/35036572>, 2000.

Bogard, M. J., Del Giorgio, P. A., Boutet, L., Chaves, M. C. G., Prairie, Y. T., Merante, A., and Derry, A. M.: Oxic water
column methanogenesis as a major component of aquatic CH₄ fluxes, *Nature communications*, 5, 5350,
<https://doi.org/10.1038/ncomms6350>, 2014.

1015 Borges, A. V., Champenois, W., Gypens, N., Delille, B., and Harlay, J.: Massive marine methane emissions from near-shore
shallow coastal areas, *Scientific reports*, 6, 27908, <https://doi.org/10.1038/srep27908>, 2016.

Borges, A. V., Speeckaert, G., Champenois, W., Scranton, M. I., and Gypens, N.: Productivity and Temperature as Drivers
of Seasonal and Spatial Variations of Dissolved Methane in the Southern Bight of the North Sea, *Ecosystems*, 21, 583–599,
<https://doi.org/10.1007/s10021-017-0171-7>, 2018.

1020 Brisch, A.: Erkundung von Torfmächtigkeit und Vegetation in zwei potenziellen Wiedervernässungsgebieten bei Rambin
und Grosow (Rügen), Unpublished expert opinion by Naturschutzzstiftung Deutsche Ostsee, 2015.

Bubier, J., Crill, P., Mosedale, A., Frolking, S., and Linder, E.: Peatland responses to varying interannual moisture
conditions as measured by automatic CO₂ chambers, *Global Biogeochem. Cycles*, 17, 1-35,
<https://doi.org/10.1029/2002GB001946>, 2003.

1025 Burgin, A. J. and Groffman, P. M.: Soil O₂ controls denitrification rates and N₂O yield in a riparian wetland, *J. Geophys. Res.*, 117, 1–15, <https://doi.org/10.1029/2011JG001799>, 2012.

Cabezas, A., Gelbrecht, J., Zwirnmann, E., Barth, M., and Zak, D.: Effects of degree of peat decomposition, loading rate and
temperature on dissolved nitrogen turnover in rewetted fens, *Soil Biology and Biochemistry*, 48, 182–191,
<https://doi.org/10.1016/j.soilbio.2012.01.027>, 2012.

1030 Capone, D. G. and Kiene, R. P.: Comparison of microbial dynamics in marine and freshwater sediments: Contrasts in
anaerobic carbon catabolism, *Limnol. Oceanogr.*, 33, 725–749, <https://doi.org/10.4319/lo.1988.33.4part2.0725>, 1988.

Carter, B. R., Radich, J. A., Doyle, H. L., and Dickson, A. G.: An automated system for spectrophotometric seawater pH
measurements, *Limnol. Oceanogr. Methods*, 11, 16–27, <https://doi.org/10.4319/lom.2013.11.16>, 2013.

1035 Chmura, G. L., Kellman, L., and Guntenspergen, G. R.: The greenhouse gas flux and potential global warming feedbacks of
a northern macrotidal and microtidal salt marsh, *Environ. Res. Lett.*, 6, 1–6, <https://doi.org/10.1088/1748-9326/6/4/044016>,
2011.

Chmura, G. L., Kellman, L., van Ardenne, L., and Guntenspergen, G. R.: Greenhouse Gas Fluxes from Salt Marshes
Exposed to Chronic Nutrient Enrichment, *PloS one*, 11, 1-13, <https://doi.org/10.1371/journal.pone.0149937>, 2016.

Couwenberg, J., Thiele, A., Tanneberger, F., Augustin, J., Bärisch, S., Dubovik, D., Liashchynskaya, N., Michaelis, D.,
1040 Minke, M., Skuratovich, A., and Joosten, H.: Assessing greenhouse gas emissions from peatlands using vegetation as a proxy, *Hydrobiologia*, 674, 67–89, <https://doi.org/10.1007/s10750-011-0729-x>, 2011.

Damm, E., Helmke, E., Thoms, S., Schauer, U., Nöthig, E., Bakker, K., and Kiene, R. P.: Methane production in aerobic oligotrophic surface water in the central Arctic Ocean, *Biogeosciences*, 7, 1099–1108, <https://doi.org/10.5194/bg-7-1099-2010>, 2010.

1045 Danevčič, T., Mandic-Mulec, I., Stres, B., Stopar, D., and Hacin, J.: Emissions of CO₂, CH₄ and N₂O from Southern European peatlands, *Soil Biology and Biochemistry*, 42, 1437–1446, <https://doi.org/10.1016/j.soilbio.2010.05.004>, 2010.

Dean, J. F., Middelburg, J. J., Röckmann, T., Aerts, R., Blauw, L. G., Egger, M., Jetten, M. S. M., Jong, A. E. E. de, Meisel, O. H., Rasigraf, O., Slomp, C. P., in't Zandt, M. H., and Dolman, A. J.: Methane Feedbacks to the Global Climate System in a Warmer World, *Rev. Geophys.*, 56, 207–250, <https://doi.org/10.1002/2017RG000559>, 2018.

1050 Dickson, A. and Riley, J.: The estimation of acid dissociation constants in seawater media from potentiometric titrations with strong base. I. The ionic product of water — Kw, *Marine Chemistry*, 7, 89–99, [https://doi.org/10.1016/0304-4203\(79\)90001-X](https://doi.org/10.1016/0304-4203(79)90001-X), 1979.

Dickson, A. G.: Standard potential of the reaction: AgCl(s) + 1/2H₂(g) = Ag(s) + HCl(aq), and the standard acidity constant of the ion HSO₄⁻ in synthetic sea water from 273.15 to 318.15 K, *The Journal of Chemical Thermodynamics*, 22, 113–127, 1055 [https://doi.org/10.1016/0021-9614\(90\)90074-Z](https://doi.org/10.1016/0021-9614(90)90074-Z), 1990.

Dickson, A. G., Sabine, C. L. and Christian, J. R. (Eds.): *Guide to best practices for ocean CO₂ measurements*, North Pacific Marine Science Organization, 2007.

Dlugokencky, E., Crotwell, A., Mund, J., Crotwell, M., and Thoning, K.: Atmospheric Methane Dry Air Mole Fractions from the NOAA ESRL Carbon Cycle Cooperative Global Air Sampling Network, 1983–2018, <https://doi.org/10.15138/wkgj-f215>, 2019b.

1060 Dlugokencky, E., Crotwell, A., Mund, J., Crotwell, M., and Thoning, K.: Atmospheric Methane Dry Air Mole Fractions from the NOAA ESRL Carbon Cycle Cooperative Global Air Sampling Network, 1983–2018, <https://doi.org/10.15138/VNCZ-M766>, 2019a.

Duhamel, S., Nogaro, G., and Steinman, A. D.: Effects of water level fluctuation and sediment–water nutrient exchange on phosphorus biogeochemistry in two coastal wetlands, *Aquat Sci*, 79, 57–72, <https://doi.org/10.1007/s00027-016-0479-y>, 2017.

Edler, L.: *Recommendations on Methods for Marine Biological Studies in the Baltic Sea: Phytoplankton and chlorophyll*, Baltic Marine Biologists;,, 1979.

Fiedler, J., Fuß, R., Glatzel, S., Hagemann, U., Huth, V., Jordan, S., Jurasinski, G., Kutzbach, L., Maier, M., Schäfer, K.,
1070 Weber, T., and Weymann, D.: Best Practice Guideline Measurement of carbon dioxide, methane and nitrous oxide fluxes
between soil-vegetation-systems and the atmosphere using non-steady state chambers, <https://doi.org/10.23689/fidgeo-5422>,
2022.

Fisher, J. and Acreman, M. C.: Wetland nutrient removal: a review of the evidence, *Hydrol. Earth Syst. Sci.*, 8, 673–685,
<https://doi.org/10.5194/hess-8-673-2004>, 2004.

1075 Flessa, H., Wild, U., Klemisch, M., and Pfadenhauer, J.: Nitrous oxide and methane fluxes from organic soils under
agriculture, 49, 1998.

Fox, J. and Weisberg, S.: An {R} Companion to Applied Regression, Third Edition. Thousand Oaks CA: Sage,
<https://socialsciences.mcmaster.ca/jfox/Books/Companion/> (last access: 03 April 2022), 2019.

Franz, D., Koebisch, F., Larmanou, E., Augustin, J., and Sachs, T.: High net CO₂ and CH₄ release at a eutrophic shallow lake
1080 on a formerly drained fen, *Biogeosciences*, 13, 3051–3070, <https://doi.org/10.5194/bg-13-3051-2016>, 2016.

Gattuso, J.-P., Epitalon, J.-M., Lavigne, H., and Orr, J.: seacarb: Seawater Carbonate Chemistry, <https://CRAN.R-project.org/> <https://CRAN.R-project.org/package=seacarb> (last access: 06 February 2022), R package version 3.2.15, 2019.

Glatzel, S., Forbrich, I., Krüger, C., Lemke, S., and Gerold, G.: Environmental controls of greenhouse gas release in a
restoring peat bog in NW Germany, *Biogeosciences Discussions*, *European Geosciences*, 213–242,
1085 <https://doi.org/10.5194/bgd-5-213-2008>, 2008.

Glatzel, S. and Stahr, K.: Methane and nitrous oxide exchange in differently fertilised grassland in southern Germany, *Plant
and Soil*, 231, 21–35, 2001.

Goldberg, S. D., Knorr, K.-H., Blodau, C., Lischeid, G., and Gebauer, G.: Impact of altering the water table height of an
acidic fen on N₂O and NO fluxes and soil concentrations, *Global change biology*, 16, 220–233,
1090 <https://doi.org/10.1111/j.1365-2486.2009.02015.x>, 2010.

Grasshoff, K., Kremling, K., and Ehrhardt, M.: Methods of Seawater Analysis, 2009.

Grolemund, G. and Wickham, H.: Dates and Times Made Easy with lubridate. *Journal of Statistical Software*,
<https://www.jstatsoft.org/v40/i03/> (last access: 03 April 2022), 2011.

Hahn, J., Köhler, S., Glatzel, S., and Jurasinski, G.: Methane Exchange in a Coastal Fen in the First Year after Flooding-A
1095 Systems Shift, *PloS one*, 10, 1-25, <https://doi.org/10.1371/journal.pone.0140657>, 2015.

Hahn-Schöfl, M., Zak, D., Minke, M., Gelbrecht, J., Augustin, J., and Freibauer, A.: Organic sediment formed during
inundation of a degraded fen grassland emits large fluxes of CH₄ and CO₂, *Biogeosciences*, 8, 1539–1550,
<https://doi.org/10.5194/bg-8-1539-2011>, 2011.

1100 Harpenslager, S. F., van den Elzen, E., Kox, M. A., Smolders, A. J., Ettwig, K. F., and Lamers, L. P.: Rewetting former agricultural peatlands: Topsoil removal as a prerequisite to avoid strong nutrient and greenhouse gas emissions, *Ecological Engineering*, 84, 159–168, <https://doi.org/10.1016/j.ecoleng.2015.08.002>, 2015.

HELCOM: HELCOM Guidelines for the annual and periodical compilation and reporting of waterborne pollution inputs to the Baltic Sea (PLC-Water), http://nest.su.se/helcom_plc/ (last access 17 December 2021), HELCOM, 2019.

1105 Heyer, J. and Berger, U.: Methane Emission from the Coastal Area in the Southern Baltic Sea, *Estuarine, Coastal and Shelf Science*, 51, 13–30, <https://doi.org/10.1006/ecss.2000.0616>, 2000.

Hogan, D. M., Jordan, T. E., and Walbridge, M. R.: Phosphorus retention and soil organic carbon in restored and natural freshwater wetlands, *Wetlands*, 24, 573–585, [https://doi.org/10.1672/0277-5212\(2004\)024\[0573:PRASOC\]2.0.CO;2](https://doi.org/10.1672/0277-5212(2004)024[0573:PRASOC]2.0.CO;2), 2004.

1110 Holz, R., Herrmann, C., and Müller-Motzfeld, G.: Vom Polder zum Ausdeichungsgebiet: Das Projekt Karrendorfer Wiesen und die Zukunft der Küstenüberflutungsgebiete in Mecklenburg-Vorpommern, *Natur und Naturschutz in MV, Schriftenreihe des Institutes für Landschaftsökologie und Naturschutz Greifswald*, Band 32, 1996.

Joosten, H. and Clarke, D.: Wise use of mires and peatlands, *Background and principles including a framework for decision-making*, 2002.

Jørgensen, B. B. (Ed.): *Bacteria and Marine Biogeochemistry*, in: *Marine Geochemistry*, https://doi.org/10.1007/3-540-32144-6_5, 2006.

1115 Jørgensen, C. J. and Elberling, B.: Effects of flooding-induced N₂O production, consumption and emission dynamics on the annual N₂O emission budget in wetland soil, *Soil Biology and Biochemistry*, 53, 9–17, <https://doi.org/10.1016/j.soilbio.2012.05.005>, 2012.

Jurasinski, G., Günther, A. B., Huth, V., Couwenberg, J., and Glatzel, S.: Paludiculture – productive use of wet peatlands., *Ecosystem services provided by paludiculture – Greenhouse gas emissions*, 79–94, 2016.

1120 Jurasinski, G., Janssen, M., Voss, M., Böttcher, M. E., Brede, M., Burchard, H., Forster, S., Gosch, L., Gräwe, U., Gründling-Pfaff, S., Haider, F., Ibenthal, M., Karow, N., Karsten, U., Kreuzburg, M., Lange, X., Leinweber, P., Massmann, G., Ptak, T., Rezanezhad, F., Rehder, G., Romoth, K., Schade, H., Schubert, H., Schulz-Vogt, H., Sokolova, I. M., Strehse, R., Unger, V., Westphal, J., and Lennartz, B.: Understanding the Coastal Ecocline: Assessing Sea–Land Interactions at Non-tidal, Low-Lying Coasts Through Interdisciplinary Research, *Front. Mar. Sci.*, 5, <https://doi.org/10.3389/fmars.2018.00342>, 2018.

1125 Jurasinski, G., Koebisch, F., Guenther, A., and Beetz, S.: Flux rate calculation from dynamic closed chamber measurements., <https://CRAN.R-project.org/package=flux> (last access: 06 February 2022), R package version 0.3-0, 2014.

Kaat, A. and Joosten, H.: *Factbook for UNFCCC policies on peat carbon emissions*, 2009.

Kandel, T. P., Lærke, P. E., Hoffmann, C. C., and Elsgaard, L.: Complete annual CO₂, CH₄, and N₂O balance of a temperate riparian wetland 12 years after rewetting, *Ecological Engineering*, 127, 527–535, 1130 <https://doi.org/10.1016/j.ecoleng.2017.12.019>, 2019.

Knittel, K. and Boetius, A.: Anaerobic oxidation of methane: progress with an unknown process, *Annual review of microbiology*, 63, 311–334, <https://doi.org/10.1146/annurev.micro.61.080706.093130>, 2009.

Koebsch, F., Glatzel, S., Hofmann, J., Forbrich, I., and Jurasinski, G.: CO₂ exchange of a temperate fen during the conversion from moderately rewetting to flooding, *J. Geophys. Res. Biogeosci.*, 118, 940–950, 1135 <https://doi.org/10.1002/jgrg.20069>, 2013.

Koebsch, F., Gottschalk, P., Beyer, F., Wille, C., Jurasinski, G., and Sachs, T.: The impact of occasional drought periods on vegetation spread and greenhouse gas exchange in rewetted fens, *Philosophical transactions of the Royal Society of London. Series B, Biological sciences*, 375, 20190685, <https://doi.org/10.1098/rstb.2019.0685>, 2020.

Koebsch, F., Jurasinski, G., Koch, M., Hofmann, J., and Glatzel, S.: Controls for multi-scale temporal variation in ecosystem methane exchange during the growing season of a permanently inundated fen, *Agricultural and Forest Meteorology*, 204, 94–105, <https://doi.org/10.1016/j.agrformet.2015.02.002>, 2015.

Koebsch, F., Winkel, M., Liebner, S., Liu, B., Westphal, J., Schmiedinger, I., Spitz, A., Gehre, M., Jurasinski, G., Köhler, S., Unger, V., Koch, M., Sachs, T., and Böttcher, M. E.: Sulfate deprivation triggers high methane production in a disturbed 1145 and rewetted coastal peatland, *Biogeosciences*, 16, 1937–1953, <https://doi.org/10.5194/bg-16-1937-2019>, 2019.

Kool, D. M., Dolfig, J., Wrage, N., and van Groenigen, J. W.: Nitrifier denitrification as a distinct and significant source of nitrous oxide from soil, *Soil Biology and Biochemistry*, 43, 174–178, <https://doi.org/10.1016/j.soilbio.2010.09.030>, 2011.

Kreyling, J., Tanneberger, F., Jansen, F., van der Linden, S., Aggenbach, C., Blüml, V., Couwenberg, J., Emsens, W.-J., Joosten, H., Klimkowska, A., Kotowski, W., Kozub, L., Lennartz, B., Liczner, Y., Liu, H., Michaelis, D., Oehmke, C., 1150 Parakenings, K., Pleyl, E., Poyda, A., Raabe, S., Röhl, M., Rücker, K., Schneider, A., Schrautzer, J., Schröder, C., Schug, F., Seeber, E., Thiel, F., Thiele, S., Tiemeyer, B., Timmermann, T., Urich, T., van Diggelen, R., Vegelin, K., Verbruggen, E., Wilmking, M., Wrage-Mönnig, N., Wolejko, L., Zak, D., and Jurasinski, G.: Rewetting does not return drained fen peatlands to their old selves, *Nature communications*, 12, 5693, <https://doi.org/10.1038/s41467-021-25619-y>, 2021.

Kuliński, K., Rehder, G., Asmala, E., Bartosova, A., Carstensen, J., Gustafsson, B., Hall, P. O. J., Humborg, C., Jilbert, T., 1155 Jürgens, K., Meier, H. E. M., Müller-Karulis, B., Naumann, M., Olesen, J. E., Savchuk, O., Schramm, A., Slomp, C. P., Sofiev, M., Sobek, A., Szymczyha, B., and Undeman, E.: Biogeochemical functioning of the Baltic Sea, *Earth Syst. Dynam.*, 13, 633–685, <https://doi.org/10.5194/esd-13-633-2022>, 2022.

Kuliński, K., Schneider, B., Hammer, K., Machulik, U., and Schulz-Bull, D.: The influence of dissolved organic matter on the acid-base system of the Baltic Sea, *Journal of Marine Systems*, 132, 106–115, 1160 <https://doi.org/10.1016/j.jmarsys.2014.01.011>, 2014.

Kuliński, K., Schneider, B., Szymczyha, B., and Stokowski, M.: Structure and functioning of the acid-base system in the Baltic Sea, *Earth Syst. Dynam.*, 8, 1107–1120, <https://doi.org/10.5194/esd-8-1107-2017>, 2017.

Lamers, L. P., Smolders, A. J., and Roelofs, J. G.: The restoration of fens in the Netherlands, *Hydrobiologia*, 478, 107–130, <https://doi.org/10.1023/A:1021022529475>, 2002.

1165 Lennartz, B. and Liu, H.: Hydraulic Functions of Peat Soils and Ecosystem Service, *Front. Environ. Sci.*, 7, <https://doi.org/10.3389/fenvs.2019.00092>, 2019.

Leppelt, T., Dechow, R., Gebbert, S., Freibauer, A., Lohila, A., Augustin, J., Drösler, M., Fiedler, S., Glatzel, S., Höper, H., Järveoja, J., Lærke, P. E., Maljanen, M., Mander, Ü., Mäkiranta, P., Minkkinen, K., Ojanen, P., Regina, K., and Strömgren, M.: Nitrous oxide emission budgets and land-use-driven hotspots for organic soils in Europe, *Biogeosciences*, 11, 6595–1170 6612, <https://doi.org/10.5194/bg-11-6595-2014>, 2014.

Liu, H. and Lennartz, B.: Short Term Effects of Salinization on Compound Release from Drained and Restored Coastal Wetlands, *Water*, 11, 1549, <https://doi.org/10.3390/w11081549>, 2019.

Liu, H., Zak, D., Rezanezhad, F., and Lennartz, B.: Soil degradation determines release of nitrous oxide and dissolved organic carbon from peatlands, *Environ. Res. Lett.*, 14, 94009, <https://doi.org/10.1088/1748-9326/ab3947>, 2019.

1175 Livingston, G. P. and Hutchinson, G.: Enclosure-based measurement of trace gas exchange: applications and sources of error., In: Matson, P.A. and Harris, R.C., Eds., *Biogenic trace gases: measuring emissions from soil and water.*, Blackwell Science Ltd., Oxford, UK., 14–51, 1995.

Löffler, A., Schneider, B., Perttilä, M., and Rehder, G.: Air–sea CO₂ exchange in the Gulf of Bothnia, Baltic Sea, *Continental Shelf Research*, 37, 46–56, <https://doi.org/10.1016/j.csr.2012.02.002>, 2012.

1180 Martikainen, P. J., Nykänen, H., Crill, P., and Silvola, J.: Effect of a lowered water table on nitrous oxide fluxes from northern peatlands, *Nature*, 366, 51–53, <https://doi.org/10.1038/366051a0>, 1993.

Millero, F. J.: Carbonate constants for estuarine waters, *Mar. Freshwater Res.*, 61, 139, <https://doi.org/10.1071/MF09254>, 2010.

1185 Minkkinen, K., Ojanen, P., Koskinen, M., and Penttilä, T.: Nitrous oxide emissions of undrained, forestry-drained, and rewetted boreal peatlands, *Forest Ecology and Management*, 478, 118494, <https://doi.org/10.1016/j.foreco.2020.118494>, 2020.

Moore, T. R., Roulet, N. T., and Waddington, J. M.: Uncertainty in Predicting the Effect of Climatic Change on the Carbon Cycling of Canadian Peatlands, *Climatic Change*, 40, 229–245, <https://doi.org/10.1023/A:1005408719297>, 1998.

1190 Moseman-Valtierra, S., Gonzalez, R., Kroeger, K. D., Tang, J., Chao, W. C., Crusius, J., Bratton, J., Green, A., and Shelton, J.: Short-term nitrogen additions can shift a coastal wetland from a sink to a source of N_2O , *Atmospheric Environment*, 45, 4390–4397, <https://doi.org/10.1016/j.atmosenv.2011.05.046>, 2011.

Müller, J. D., Bastkowski, F., Sander, B., Seitz, S., Turner, D. R., Dickson, A. G., and Rehder, G.: Metrology for pH Measurements in Brackish Waters—Part 1: Extending Electrochemical pHT Measurements of TRIS Buffers to Salinities 5–20, *Front. Mar. Sci.*, 5, <https://doi.org/10.3389/fmars.2018.00176>, 2018.

1195 Müller, J. D. and Rehder, G.: Metrology of pH Measurements in Brackish Waters—Part 2: Experimental Characterization of Purified meta-Cresol Purple for Spectrophotometric pHT Measurements, *Front. Mar. Sci.*, 5, <https://doi.org/10.3389/fmars.2018.00177>, 2018.

Müller, J. D., Schneider, B., and Rehder, G.: Long-term alkalinity trends in the Baltic Sea and their implications for CO₂-induced acidification, *Limnol. Oceangr.*, 61, 1984–2002, <https://doi.org/10.1002/lno.10349>, 2016.

1200 Neubauer, S. C., Franklin, R. B., and Berrier, D. J.: Saltwater intrusion into tidal freshwater marshes alters the biogeochemical processing of organic carbon, *Biogeosciences*, 10, 8171–8183, <https://doi.org/10.5194/bg-10-8171-2013>, 2013.

Oertel, C., Matschullat, J., Zurba, K., Zimmermann, F., and Erasmi, S.: Greenhouse gas emissions from soils—A review, *Geochemistry*, 76, 327–352, <https://doi.org/10.1016/j.chemer.2016.04.002>, 2016.

1205 Oremland, R. S. (Ed.): The biogeochemistry of methanogenic bacteria, in: *The biology of microorganisms*. Available online at <http://pubs.er.usgs.gov/publication/70198767>, 1988.

Parish, F.: Assessment on peatlands, biodiversity and climate change, Main report, 2008.

Pedersen, T. L.: patchwork: The Composer of Plots. R package version 1.1.1, <https://CRAN.R-project.org/package=patchwork>, 2020.

1210 Petersen, S. O., Hoffmann, C. C., Schäfer, C.-M., Blicher-Mathiesen, G., Elsgaard, L., Kristensen, K., Larsen, S. E., Torp, S. B., and Greve, M. H.: Annual emissions of CH₄ and N₂O, and ecosystem respiration, from eight organic soils in Western Denmark managed by agriculture, *Biogeosciences*, 9, 403–422, <https://doi.org/10.5194/bg-9-403-2012>, 2012.

Pönisch, D. L.: Methodenentwicklung und –anwendung zur Analytik von Methan und Lachgas in Seewasser, Leibniz Institute for Baltic Sea Research Warnemünde (IOW), Master thesis, 2018.

1215 Rassamee, V., Sattayatewa, C., Pagilla, K., and Chandran, K.: Effect of oxic and anoxic conditions on nitrous oxide emissions from nitrification and denitrification processes, *Biotechnology and bioengineering*, 108, 2036–2045, <https://doi.org/10.1002/bit.23147>, 2011.

Reeburgh, W. S.: Oceanic methane biogeochemistry, *Chemical reviews*, 107, 486–513, <https://doi.org/10.1021/cr050362v>, 2007.

1220 Regina, K., Silvola, J., and Martikainen, P. J.: Short-term effects of changing water table on N_2O fluxes from peat monoliths from natural and drained boreal peatlands, *Global change biology*, 5, 183–189, <https://doi.org/10.1046/j.1365-2486.1999.00217.x>, 1999.

Richert, M., Dietrich, O., Koppisch, D., and Roth, S.: The Influence of Rewetting on Vegetation Development and Decomposition in a Degraded Fen, *Restor Ecology*, 8, 186–195, <https://doi.org/10.1046/j.1526-100x.2000.80026.x>, 2000.

1225 Roughan, B. L., Kellman, L., Smith, E., and Chmura, G. L.: Nitrous oxide emissions could reduce the blue carbon value of marshes on eutrophic estuaries, *Environ. Res. Lett.*, 13, 44034, <https://doi.org/10.1088/1748-9326/aab63c>, 2018.

Rysgaard, S., Thastum, P., Dalsgaard, T., Christensen, P. B., Sloth, N. P., and Rysgaard, S.: Effects of Salinity on NH_4^+ Adsorption Capacity, Nitrification, and Denitrification in Danish Estuarine Sediments, *Estuaries*, 22, 21, <https://doi.org/10.2307/1352923>, 1999.

1230 Sabbaghzadeh, B., Arévalo-Martínez, D. L., Glockzin, M., Otto, S., and Rehder, G.: Meridional and Cross-Shelf Variability of N_2O and CH_4 in the Eastern-South Atlantic, *J. Geophys. Res. Oceans*, 126, <https://doi.org/10.1029/2020JC016878>, 2021.

Schneider, B. and Müller, J. D.: Biogeochemical Transformations in the Baltic Sea, <https://doi.org/10.1007/978-3-319-61699-5>, 2018.

Schönheit, P., Kristjansson, J. K., and Thauer, R. K.: Kinetic mechanism for the ability of sulfate reducers to out-compete 1235 methanogens for acetate, *Archives of microbiology*, 132, 285–288, 1982.

Segarra, K. E., Comerford, C., Slaughter, J., and Joye, S. B.: Impact of electron acceptor availability on the anaerobic oxidation of methane in coastal freshwater and brackish wetland sediments, *Geochimica et Cosmochimica Acta*, 115, 15–30, <https://doi.org/10.1016/j.gca.2013.03.029>, 2013.

Segers, R. and Kengen, S.: Methane production as a function of anaerobic carbon mineralization: A process model, *Soil 1240 Biology and Biochemistry*, 30, 1107–1117, [https://doi.org/10.1016/S0038-0717\(97\)00198-3](https://doi.org/10.1016/S0038-0717(97)00198-3), 1998.

Steinle, L., Maltby, J., Treude, T., Kock, A., Bange, H. W., Engbersen, N., Zopfi, J., Lehmann, M. F., and Niemann, H.: Effects of low oxygen concentrations on aerobic methane oxidation in seasonally hypoxic coastal waters, *Biogeosciences*, 14, 1631–1645, <https://doi.org/10.5194/bg-14-1631-2017>, 2017.

Steinmuller, H. E. and Chambers, L. G.: Can Saltwater Intrusion Accelerate Nutrient Export from Freshwater Wetland Soils?
1245 An Experimental Approach, *Soil Sci. Soc. Am. j.*, 82, 283–292, <https://doi.org/10.2136/sssaj2017.05.0162>, 2018.

Strack, M. (Ed.): Peatlands and climate change, *Internat. Peat Soc.*, 2008.

Succow, M. and Joosten, H. (Eds.): Landschaftsökologische Moorkunde, E. Schweizerbart'sche Verlagsbuchhandlung (Nägele u. Obermiller), 2001.

Thomas, H. and Schneider, B.: The seasonal cycle of carbon dioxide in Baltic Sea surface waters, *Journal of Marine Systems*, 22, 53–67, [https://doi.org/10.1016/S0924-7963\(99\)00030-5](https://doi.org/10.1016/S0924-7963(99)00030-5), 1999.

1250 Treude, T., Krüger, M., Boetius, A., and Jørgensen, B. B.: Environmental control on anaerobic oxidation of methane in the gassy sediments of Eckernförde Bay (German Baltic), *Limnol. Oceangr.*, 50, 1771–1786, <https://doi.org/10.4319/lo.2005.50.6.1771>, 2005.

van de Riet, B. P., Hefting, M. M., and Verhoeven, J. T. A.: Rewetting Drained Peat Meadows: Risks and Benefits in Terms of Nutrient Release and Greenhouse Gas Exchange, *Water Air Soil Pollut. (Water, Air, & Soil Pollution)*, 224, 1255 <https://doi.org/10.1007/s11270-013-1440-5>, 2013.

Voss, M., Deutsch, B., Liskow, I., Pastuszak, M., Schulte, U., and Sitek, S.: Nitrogen retention in the Szczecin Lagoon, Baltic Sea, *Isotopes in environmental and health studies*, 46, 355–369, <https://doi.org/10.1080/10256016.2010.503895>, 2010.

Wang, M., Liu, H., and Lennartz, B.: Microtopography effects on carbon accumulation and nutrient release from rewetted 1260 coastal wetlands., AGU2021 Fall Meeting, 2021.

Wanninkhof, R.: Relationship between wind speed and gas exchange over the ocean revisited, *Limnol. Oceanogr. Methods*, 12, 351–362, <https://doi.org/10.4319/lom.2014.12.351>, 2014.

Weiss, R. F. and Price, B. A.: Nitrous oxide solubility in water and seawater, *Marine Chemistry*, 8, 347–359, 1265 [https://doi.org/10.1016/0304-4203\(80\)90024-9](https://doi.org/10.1016/0304-4203(80)90024-9), 1980.

Wickham, H., Averick, M., Bryan, J., Chang, W., McGowan, L. D., François, R., Grolemund, G., Hayes, A., Henry, L., Hester, J., Kuhn, M., Pedersen, T. L., Miller, E., Bache, S. M., Müller, K., Ooms, J., Robinson, D., Seidel, D. P., Spinu, V., Takahashi, K., Vaughan, D., Wilke, C., Woo, K., and Yutani, H.: Welcome to the tidyverse. *Journal of Open Source Software*, <https://doi.org/10.21105/joss.01686>, 2019.

Wolf-Gladrow, D. A., Zeebe, R. E., Klaas, C., Kötzinger, A., and Dickson, A. G.: Total alkalinity: The explicit conservative 1270 expression and its application to biogeochemical processes, *Marine Chemistry*, 106, 287–300, <https://doi.org/10.1016/j.marchem.2007.01.006>, 2007.

Zak, D. and Gelbrecht, J.: The mobilisation of phosphorus, organic carbon and ammonium in the initial stage of fen rewetting (a case study from NE Germany), *Biogeochemistry*, 85, 141–151, <https://doi.org/10.1007/s10533-007-9122-2>, 2007.

1275 Zak, D., Meyer, N., Cabezas, A., Gelbrecht, J., Mauersberger, R., Tiemeyer, B., Wagner, C., and McInnes, R.: Topsoil removal to minimize internal eutrophication in rewetted peatlands and to protect downstream systems against phosphorus pollution: A case study from NE Germany, *Ecological Engineering*, 103, 488–496, <https://doi.org/10.1016/j.ecoleng.2015.12.030>, 2017.

Zielinski, T., Sagan, I. and Surosz, W. (Eds.): *Interdisciplinary Approaches for Sustainable Development Goals*, Springer International Publishing, <https://doi.org/10.1007/978-3-319-71788-3>, 2018.